A 25,000-year record of climate and vegetation change from the southwestern Cape coast, South Africa

Lynne J. Quick[1], Brian M. Chase[2,3], Andrew S. Carr[4], Manuel Chevalier[5], B. Adriaan Grobler[1], Michael E. Meadows[3,6,7]

[1]*African Centre for Coastal Palaeoscience, Nelson Mandela University, Port Elizabeth, Eastern Cape 6031, South Africa*

[2]*Institut des Sciences de l'Evolution-Montpellier (ISEM), University of Montpellier, Centre National de la Recherche Scientifique (CNRS), EPHE, IRD, Montpellier, France. (ORCID: 0000-0001-6987-1291)*

[3]*Department of Environmental and Geographical Science, University of Cape Town, South Lane, Upper Campus, 7701 Rondebosch, South Africa*

[4]*School of Geography, Geology and the Environment, University of Leicester, University Road, Leicester LE1 7RH, UK*

[5]*Institut für Geowissenschaften und Meteorologie, Rheinische Friedrich-Wilhelms-Universität Bonn, Auf dem Hügel 20, 53121 Bonn, Germany (ORCID: 0000- 002-8183-9881)*

[6]*School of Geographic Sciences, East China Normal University, 500 Dongchuan Road, Shanghai 200241, PR China*

[7]*College of Geography and Environmental Sciences, Zhejiang Normal University, Jinhua 321004, China*

Corresponding Author:

Lynne Quick[1]

Email address: lynne.j.quick@gmail.com ; telephone: +27(0)41 504 4105

Abstract

The southwestern Cape of South Africa is a particularly dynamic region in terms of long-term climate change. We analysed fossil pollen from a 25,000-year sediment core taken from a near-coastal wetland

at Pearly Beach that revealed that distinct changes in vegetation composition occurred along the southwestern Cape coast. From these changes, considerable variability in temperature and moisture availability are inferred. Consistent with indications from elsewhere in southwestern Africa, variability in Atlantic meridional overturning circulation (AMOC) was identified as a strong determinant of regional climate change. At Pearly Beach this resulted in phases of relatively drier conditions (~24-22.5 cal ka BP and ~22-18 cal ka BP) demarcated by brief phases of increased humidity from ~24.5-24 cal ka BP and 22.5-22 cal ka BP. During glacial Termination I (~19 – 11.7 ka), a marked increase in coastal thicket pollen from ~18.5-15.0 cal ka BP indicates a substantial increase in moisture availability, coincident, and likely associated with, slowing AMOC and a build-up of heat in the southern Atlantic. With clear links to glacial and deglacial Earth system dynamics and perturbations, the Pearly Beach record represents an important new contribution to a growing body of data, providing insights into the patterns and mechanisms of southwestern African climate change.

Keywords

Last Glacial Maximum; Heinrich stadial 1; Atlantic meridional overturning circulation; climate change; vegetation dynamics; South Africa

INTRODUCTION

The southwestern Cape of South Africa is a particularly dynamic region in terms of long-term climate change as it is situated at the nexus of the three dominant climate systems in southern Africa: the South Atlantic anticyclone, the temperate westerlies and the tropical easterlies (Tyson, 1986; Taljaard, 1996; Tyson and Preston-Whyte, 2000; Chase and Meadows, 2007). While most of the subcontinent experiences summer rainfall as a result of perturbations in the tropical easterlies, the southwestern Cape presently receives the majority of its rainfall during the austral winter, when the southern westerly storm track migrates northward (Tyson, 1986; Taljaard, 1996; Tyson and Preston-Whyte, 2000). In contrast, during

51 the austral summer, the westerlies and the South Atlantic Anticyclone shift southward limiting the
52 influence of both frontal systems and tropical moisture sources (Tyson and Preston-Whyte, 2000; Reason
53 et al., 2006). These spatially-distinct precipitation patterns led to the classification of the winter rainfall
54 zone (WRZ) (*sensu* Chase and Meadows, 2007; >66% of annual precipitation in winter), the summer
55 rainfall zone (SRZ; >66% of annual precipitation in summer) and a transitional zone of limited seasonality
56 between the WRZ and SRZ, the aseasonal or year-round rainfall zone (ARZ) (Fig. 1).

57 The southwestern Cape is also where the warm Agulhas Current and the cold Benguela Current
58 meet and, the region is thus also particularly dynamic from an oceanographic perspective. Both currents
59 are key components of the global ocean "conveyor belt" (thermohaline circulation) (Lutjeharms, 1996;
60 Rahmstorf, 2006) and therefore contribute not only to climatic variability within the southwestern Cape
61 but also play a role in global climate dynamics (Walker, 1990; Walker and Shillington, 1990; Cohen and
62 Tyson, 1995; Reason, 2001; Biastoch et al., 2009; Beal et al., 2011).

63 The climatic setting of the southwestern Cape has played an important part in the development
64 of the vegetation of the Cape Floristic Region (CFR) and is thought to have fostered the region's
65 extraordinary botanical diversity (Goldblatt, 1978; Linder et al., 1992; Cowling and Lombard, 2002; Linder,
66 2005; Bradshaw and Cowling, 2014; Cowling et al., 2015). While long-term climatic stability during the
67 Pliocene and Pleistocene is hypothesised to be one of the key factors for the diversification of the Cape
68 flora (Cowling et al., 1997; Cowling and Lombard, 2002; Linder, 2005; Bergh and Cowling, 2014; Cowling
69 et al., 2015), little direct evidence is available. Furthermore, species diversity within the CFR is not
70 homogeneous and at finer spatial and temporal scales the concept of climatic stability driving diversity
71 and species richness becomes more complex (Cowling, 1992; Cowling et al., 1997; Cowling and Lombard,
72 2002). Palaeoclimatic records from the western montane region of the CFR provide evidence for steep

palaeoenvironmental gradients and highlight the need for more research to be conducted to assess the role of palaeoclimatic change in biodiversity patterns (Chase et al., 2019a).

Despite the challenges of conducting Quaternary paleoenvironmental studies in arid – semi-arid areas (see Chase and Meadows, 2007), considerable progress has been made over the last decade in terms of the generation of high-resolution palaeoclimatic records for the southwestern and southern Cape regions (e.g. Neumann et al., 2011; Stager et al., 2012; Chase et al., 2013; Valsecchi et al., 2013; Chase et al., 2015a; Quick et al., 2018; Wündsch et al., 2018; Chase et al., 2019a; Chase et al., 2020; Kirsten et al., 2020). This emerging regional dataset is enabling a more refined understanding of the spatial and temporal complexity of climate and vegetation responses to a range of forcing mechanisms, and suggests that substantial variability in inferred climatic trends/trajectories occurs across relatively short distances (e.g. Chase et al., 2015a; Chase et al., 2017; Chase and Quick, 2018; Chase et al., 2020). Even though more – and indeed more detailed – records are now available, most of these records only cover the Holocene (11.7 – 0 cal ka BP) or portions thereof. In particular, greater spatial and temporal coverage is still needed to fully document the Last Glacial Maximum (LGM; 19 – 26.5 ka (Clark et al., 2009))and last glacial termination (Termination I; the period from the end of the Last Glacial Maximum to the early Holocene, ~19 – 11.7 ka).

During Termination I, one of the primary internal drivers of global change was variability in Atlantic meridional overturning circulation (AMOC), a key component of the thermohaline circulation (Mix et al., 1986; Crowley, 1992; Broecker, 1998; Stocker, 1998; Stocker and Johnsen, 2003). AMOC transports heat from the Southern Hemisphere to the North Atlantic basin. Perturbations in the strength of the AMOC thus impact climate in both hemispheres, with stronger AMOC resulting in net cooling (warming) in the Southern (Northern) Hemisphere, and weaker AMOC resulting in a build-up of heat in the Southern Hemisphere while the Northern Hemisphere cools, a dynamic referred to as the bipolar seesaw (Broecker,

1998; Stocker and Johnsen, 2003). Massive ice and freshwater discharges in the North Atlantic, known as Heinrich events, exerted a significant influence on AMOC, resulting, for example, in its near shut-down during Heinrich stadial 1 (HS1; ~18-14.6 ka) (Broecker, 1998; McManus et al., 2004; Ritz et al., 2013; Ng et al., 2018; Bendle et al., 2019).

In the southwest African sector, the influence of weaker AMOC is manifested in a general warming of southeast Atlantic sea-surface temperatures (SSTs) (Kim and Schneider, 2003; Farmer et al., 2005), a poleward shift of the Subtropical Front (Barker et al., 2009), and thus likely an increase in Agulhas leakage (Gordon, 1986; Peeters et al., 2004; Caley et al., 2012; Rühs et al., 2019). As an example, the abrupt slow-down in AMOC during HS1 is consistent as the underlying driver for the distinct humid phase registered at sites along the western continental margin in the Namib Desert (Lim et al., 2016; Chase et al., 2019b) and the Cederberg mountains in the southwestern Cape (Chase et al., 2015a), as well as further afield in the continental interior (Chase et al., 2017; Chevalier and Chase, 2015). It remains to be determined, however, how these changes in AMOC affected Africa's southern/southwestern Cape coast, particularly in the context of the emerging evidence for spatial complexity in the regional climatic response (Chase and Quick, 2018; Chase et al., 2019a; Chase et al., 2020). This brings into question the utility of the simple widely-used binary models that indicate or infer a coeval inverse relationship between the WRZ and SRZ (van Zinderen Bakker, 1976; Cockcroft et al., 1987) and thus how climate changes related to AMOC may have manifested in the region.

To investigate the potential influence of AMOC variability at the interface of the Agulhas and Benguela currents and at the margin of the WRZ, here we present a new record of fossil pollen, charcoal and sediment grain-size from a 25,000-year sediment core taken from Pearly Beach 1, a near-coastal wetland site situated on the eastern coastal boundary of the present-day WRZ (Figs. 1 and 2). Data from the core presents a rare opportunity to consider vegetation/climate responses through this major global

climate transition. The record reveals distinct changes in vegetation composition occurred along the southwestern Cape coast during the LGM, Termination I and Holocene. From these data, we infer considerable variability in temperature and moisture availability over the last 25 000 years and link these changes to glacial and interglacial boundary conditions, and particularly, to the perturbations and dynamics in the Earth system that characterised the process of deglaciation.

REGIONAL SETTING

In 2007, a sediment core (Pearly Beach 1, referred to hereafter as PB1, 34° 38.880'S; 19° 30.300'E, 5 m a.s.l., 2.5 km from the current coastline (Fig. 2)) was extracted from wetlands 2 km north of the coastal town of Pearly Beach, ~200 km southeast of Cape Town. The site is situated on the boundary of the modern WRZ (*sensu* Chase and Meadows, 2007; >66% of annual precipitation falling in MJJAS), receiving 68% of its mean annual average of ~450 mm of rainfall during the winter (Climate System Analysis Group, 2021). Temperatures are moderate (monthly-averaged daily mean of 17 °C), snow has not been recorded and frost appears to be absent from the area as well.

The Pearly Beach wetland complex is situated on a low-lying undulating coastal plain that is bounded to the north by Bredasdorp Group limestone (calcarenite) ridges and Table Mountain Group sandstone outcrops of Peninsula Formation (Malan, 1989). The wetlands derive their waters from the limestone uplands to the northeast of the site via both runoff and throughflow from spring seeps. Transverse coastal dunes, currently invaded by extensive alien vegetation, stretch along the southern and western boundaries of the wetland adjacent to the ocean. Relict deflated parabolic dunes can be identified within the landscape towards the northwest and southeast of the site. The coastal platform is underlain by unconsolidated aeolian calcareous Quaternary sediments of the Strandveld Formation with partially consolidated calcrete lenses found in some patches along the coast and further inland (Gresse and Theron, 1992). Alluvial deposits characterise the wetlands of the area. On the limestone ridges, soils

142 are shallow, alkaline and calcareous, whereas the lower slopes are characterised by more acidic, colluvial
143 soils with evidence of early stages of podsolisation (Rebelo et al., 1991). The young coastal dune sands are
144 associated with deeper calcareous, alkaline soils in comparison to the soils found on the slopes.

145 ## Contemporary vegetation

146 The study area (Fig. 2) is home to the *Groot Hagelkraal* farm – a registered private nature reserve and a
147 South African Nature Foundation Natural Heritage Site. The Groot Hagelkraal area harbours six local-
148 endemic and 21 regional-endemic plant species, and has been lauded as the world's "hottest" biodiversity
149 hotspot and foremost conservation priority in the CFR (Cowling, 1996; Willis et al., 1996; Jones et al.,
150 2002). The surrounding landscape is dominated by 1) sclerophyllous, Mediterranean-type shrublands of
151 the fynbos biome, found on both the lowlands and uplands, 2) subtropical thickets that occupy parts of
152 the near-coastal dune fields adjacent to the site, and 3) pockets of forest vegetation in more sheltered
153 sites (Cowling et al., 1988; Mucina and Rutherford, 2006). Where surface water is perennially or seasonally
154 available, lowland areas also support riparian and wetland habitats (Mustart et al., 2003).

155 The azonal vegetation associated with wetland systems around Pearly Beach and the upper
156 reaches of the Groot Hagelkraal River is broadly classified as Cape Lowland Freshwater Wetlands (Mucina
157 et al., 2006b). These systems are dominated by the reed, *Phragmites australis* (Poaceae), and the rushes
158 *Juncus kraussii* and *J. capensis* (Juncaceae). Sedges, especially *Ficinia nodosa* (Cyperaceae), form dense
159 stands along the margins of the vlei, while *Typha capensis* and *Isolepis prolifera* (Cyperaceae) inhabit the
160 open water and shallower margins, together with obligate aquatics like *Aponogeton distachyos* and
161 *Nymphaea nouchali*.

162 Three broad types of fynbos vegetation occur in the study area, each associated with a specific
163 edaphic substrate (Thwaites and Cowling, 1988). Agulhas Limestone Fynbos occurs in fragmented patches
164 inland of the Pearly Beach site on shallow, alkaline sands that accumulate in depressions over Bredasdorp

Group limestone pavements (Cowling et al., 1988; Mustart et al., 2003; Rebelo et al., 2006). This mid-high, moderately dense shrubland contains tall, emergent proteoids and is characterised by the presence of *Protea obtusifolia* and *Leucadendron meridianum*. The restioid component is poorly developed, but the widespread species *Elegia microcarpa* and *Restio leptoclados*, and the more restricted *Thamnochortus fraternus*, are typical of this fynbos type. Typical ericoid shrubs include *Aspalathus calcarea* (Fabaceae), *Metalasia calcicola* (Asteraceae), *Phylica selaginoides* and *Passerina paleacea*, as well as several local- and regional-endemic species of the Ericaceae (e.g. *Erica calciphila*) and Rutaceae (e.g. *Diosma haelkraalensis*) (Mustart et al., 2003; Rebelo et al., 2006).

Similar to Agulhas Limestone Fynbos, Agulhas Sand Fynbos is associated with Bredasdorp Group limestones, but this vegetation type occurs on deep colluvial, neutral sands that fringe the base of limestone outcrops (Cowling et al., 1988; Mustart et al., 2003; Rebelo et al., 2006). Overstorey proteoids that characterise this vegetation type are *Protea susannae* and *Leucadendron coniferum*. Typical ericoid shrubs include *Erica discolor*, *E. plukenetii* subsp. *lineata*, *Metalasia densa* and *Passerina corymbosa*, as well as the Hagelkraal-endemic, *Spatalla ericoides* (Mustart et al., 2003; Rebelo et al., 2006). Commonly occurring restioids are *Elegia filacea*, *E. tectorum*, *Restio triticeus*, *Thamnochortus erectus* and *T. insignis*.

Overberg Sandstone Fynbos occurs on the rolling uplands where it is associated with deep colluvial, infertile acid sands derived from Table Mountain Group sandstones (Thwaites and Cowling, 1988; Cowling et al., 1988; Rebelo et al., 2006) (Fig. 2). *Protea compacta* is the dominant and characteristic overstorey proteoid, while *Leucadendron xanthoconus* is also common. Restioids can be locally abundant, with *Ceratocaryum argenteum*, *Hypodiscus argenteus*, *Mastersiella digitata* and *Staberoha multispicula* being typical species.

The deep, well-drained alkaline sands of coastal dunes in the study area support Overberg Dune Strandveld, a mosaic-type vegetation comprising small clumps of subtropical thicket in a matrix of

asteraceous fynbos (Cowling et al., 1988; Rebelo et al., 2006). The dune-fynbos component is dominated by non-ericaceous ericoid shrubs, especially *Acmadenia obtusata* (Rutaceae), *Agathosma collina* (Rutaceae), *Metalasia muricata* (Asteraceae)*, Muraltia satureioides* (Polygalaceae), *Passerina paleacea* and *Phylica ericoides* (Mustart et al., 2003). Restioids are not abundant in the dune fynbos; this group is typically represented by only two species, *Elegia microcarpa* and *Restio eleocharis*. A conspicuous difference between the fynbos component of Overberg Dune Strandveld and the other fynbos vegetation types occurring in the study area is the absence of proteoids in the former (Cowling et al., 1988). While subtropical thicket shrubs occur throughout Overberg Dune Strandveld, dune thicket clumps are best developed in moist, wind- and fire-protected dune slacks where their structure and composition approach that of coastal forests (see below). Characteristic dune thicket shrubs include *Carissa bispinosa* (Apocynaceae), *Euclea racemosa*, *Morella cordifolia, Myrsine africana, Lauridia tetragona* (Celastraceae), *Olea exasperata*, *Robsonodendron maritimum* (Celastraceae), *Pterocelastrus tricuspidatus* (Celastraceae) and *Searsia glauca* (Cowling et al., 1988; Mustart et al., 2003; Rebelo et al., 2006).

The azonal vegetation associated with coastal strands, rocky shorelines and mobile dune cordons in the study area is classified as Cape Seashore Vegetation (Mucina et al., 2006a). Sandy areas typically host the grasses *Ehrharta villosa* and *Thinopyrum distichum* (both Poaceae), the succulent shrubs *Tetragonia decumbens* and *Carpobrotus acinaciformis* (both Aizoaceae), several herbaceous species like *Arctotheca populifolia* (Asteraceae), *Dasispermum suffriticosum* (Apiaceae), *Senecio elegans* (Asteraceae) and *Silene crassifolia* (Caryophyllaceae), and the shrubs *Hebenstreitia cordata* (Scrophulariaceae)*, Morella cordifolia* and *Passerina rigida* (Mustart et al., 2003; Mucina et al., 2006a). The more stabilised dunes half a kilometre inland of the littoral zone are predominantly vegetated by *Osteospermum moniliferum* (Asteraceae), which, together with other woody species like *Searsia crenata*, form small pockets of wind-pruned thicket. Along rocky shores, the vegetation comprises low grasslands of salt-tolerant species like *Sporobolus virginicus* and *Stenotaphrum secundatum*, or succulent herblands where *Dimorphotheca*

fruticosa (Asteraceae), *Drosanthemum intermedium* (Aizoaceae), *Mesembryanthemum vanrensburgii* (Aizoaceae) and *Plantago crassifolia* are typical.

There are small, isolated patches of Southern Coastal Forest to the west of the site which are dominated by *Sideroxylon inerme*. Other trees and shrubs present in these patches include *Cassine peragua* (Celastraceae), *Chionanthus foveolatus* (Oleaceae), *Robsonodendron maritimum* (Celastraceae), *Maytenus procumbens* (Celastraceae), *Olea capensis, Polygala myrtifolia*, *Pterocelastrus tricuspidatus* (Celastraceae) and *Tarchonanthus littoralis* (Asteraceae) (Mustart et al., 2003; Mucina and Geldenhuys, 2006).

MATERIALS AND METHODS

Chronology

The age-depth model for the PB1 core was constructed from eight radiocarbon ages (Table 1). Subsamples of approximately 1 g were taken from various positions along the PB1 core and sent to *Beta Analytic Inc* for AMS radiocarbon dating. These ages were calculated using the Libby half-life of 5568 years following Stuiver and Polach (1977). The ages were corrected for isotope fractionation using the AMS-measured $\delta^{13}C$, which accounts for both natural and machine fractionation.

The age-depth model was developed in the software package *rbacon* (v. 2.3.6; Blaauw and Christen, 2011). Using a Bayesian framework, Bacon divides the core into sections and models the accumulation rate for each section through multiple Markov Chain Monte Carlo (MCMC) iterations. The ages were calibrated with the SHCal13 data (Hogg et al., 2013).

Particle size analysis

Particle size analysis was conducted at the Department of Geography, Friedrich-Schiller-University, Jena, Germany. Subsamples of ~5 g were pre-treated to remove organic material with hydrogen peroxide (H_2O_2) while carbonates were removed with hydrochloric acid (HCl). Sodium pyrophosphate ($Na_4P_2O_7$) was added as deflocculant. The particle size distributions were detected using a Beckman Coulter LS 13 320 Laser Diffraction Particle Size Analyzer, the single wavelength Aqueous Liquid Module (ALM). Measurements were carried out in several runs until a reproducible signal was obtained.

Pollen and microcharcoal analyses

Pollen and microcharcoal subsamples (1 cm-thick) were initially taken at 5 cm intervals. This was followed by finer resolution subsampling at targeted locations along the core that were identified by the initial pollen results as representing periods of significant vegetation change.

Palynomorphs were concentrated and extracted following Moore et al. (1991) with specific adaptations for dense media separation from Nakagawa et al. (1998). This involved 30% HCl treatment to remove carbonates, 10% KOH digestion to disaggregate the samples and remove humic acids and heavy liquid mineral separation using $ZnCl_2$ to separate the pollen grains from the non-pollen matrix (Faegri and Iversen, 1989; Moore et al., 1991; Nakagawa et al., 1998). Samples were acetolysised and mounted in *Aquatex*, an aqueous mounting agent. Three slides were produced per sample and absolute pollen concentrations were calculated via the addition of *Lycopodium* spores as per Stockmarr (1973). Pollen counts of 500 grains per sample were carried out at 400x magnification for routine identification and 1000x for specific identification. Non-pollen palynomorphs (NNPs) were counted but not included in the total pollen sum. The University of Cape Town pollen reference collection and published resources (van Zinderen Bakker, 1953, 1956; van Zinderen Bakker and Coetzee, 1959; Scott, 1982) were used for the identification of pollen taxa. The pollen and microcharcoal diagram was constructed in Tilia (version

2.1.1)(Grimm, 1991) and was divided into statistically significant pollen assemblage zones based on a CONISS (Constrained Incremental Sum of Squares) (with square root transformation) analysis (Grimm, 1987).

Charcoal particles were identified and counted on the same microscope slides produced for the pollen analysis. Only particles that were black, opaque and angular were considered charcoal fragments (Patterson et al., 1987; Mooney and Tinner, 2011). Charcoal fragments were classified and counted according to two size categories based on the long axis of each fragment; 10–100 µm and >100 µm. Particles less than 75 μm^2 (or ~10 µm long) were not counted due to the risk of false identification (Mooney and Tinner, 2011). Therefore, the charcoal signal primarily relates to the regional (10–100 µm) and local (>100 µm) fire signals and excludes extra-regional fires (<10 µm). Absolute charcoal abundances were calculated in the same manner as pollen concentrations (Stockmarr, 1973).

Defining plant-climate relationships

To objectively define the plant-climate relationships associated with the Pearly Beach pollen assemblage, we used the CREST (Climate REconstruction SofTware) method and software (Chevalier et al., 2014; Chevalier, 2019). For our analyses, we used botanical data obtained from the Global Biodiversity Information Facility (GBIF) database (Global Biodiversity Information Facility, https://www.gbif.org/), specifically the curated dataset of Chevalier (2020), and we used a regional subset of the Worldclim 2 climatology (Fick and Hijmans, 2017).

RESULTS

Stratigraphy and chronology

The particle size analysis results indicate that the 250 cm core predominantly comprises sands and silty sands with three distinct zones of pale coarser-textured sands at the top (0 – 25 cm), middle (130 – 160

276 cm) and base (235 – 250 cm) of the core (Figs. 3 and 4, Appendix A). They are bounded by relatively
277 homogeneous organic-rich silty sands. The exception being a thin lens of light-coloured coarser sand
278 situated between 175 and 180 cm (Fig. 3).

279 The core spans the period ~25.3 cal ka BP to present (Fig. 3), encompassing much of the LGM (19-26.5
280 cal ka BP), Termination I (~19 - 11.7 cal ka BP) and the Holocene (11.7 - 0 cal kBP).

281 ## Pollen and microcharcoal

282 A total of 102 pollen taxa were identified from the 78 samples analysed. The pollen, non-pollen
283 palynomorphs, microcharcoal and particle size data (Fig. 4, Fig. 5, Appendix A) were divided based on
284 CONISS analysis results and assemblage variability into four pollen assemblage zones (and three
285 subzones). Pollen concentrations range between $2x10^3$ and $33x10^3$ grain g^{-1}, with peaks in concentration
286 22.5 – 19 cal ka BP and 14 – 12 cal ka BP. No pollen was preserved from 11.6 – 8.5 cal ka BP.

287 The overall assemblage is characterised by variations in fynbos taxa (e.g. Proteaceae, Ericaceae,
288 Restionaceae, *Cliffortia* and *Stoebe*-type), coastal thicket elements (such as *Euclea*, *Morella* and
289 *Canthium*[1]), succulent/drought-resistant elements (e.g. Aizoaceae, *Crassula* and *Euphorbia*) and local
290 wetland vegetation (predominantly Cyperaceae, Juncaceae and Haloragaceae) as well as more
291 cosmopolitan pollen types such as Asteraceae and Poaceae. Ericaceace pollen is most prominent at the
292 base of the sequence (pollen assemblage zone PB1-A; 25 – 21 cal ka BP), coinciding with the only
293 significant presence of *Passerina*, relatively elevated proportions of *Stoebe*-type (which includes various
294 *Stoebe* and *Elytropappus* spp.) and low percentages of Proteaceae and Restionaceae. A further
295 distinguishing feature of PB1-A is the generally greater proportions of coastal thicket taxa, particularly
296 *Euclea* and Santalaceae, as well as discrete, relatively high, peaks in *Dodonaea* and *Morella* from 22.5 –

[1] The *Canthium* pollen type includes *Canthium mundianum* which has been renamed *Afrocanthium mundianum* (Lantz and Bremer, 2004).

21.5 cal ka BP. The isolated peaks in *Dodonaea* and *Morella* coincide with a large spike in *Crassula* (14%) and a smaller peak in Aizoaceae. Just prior to this phase, the highest counts and greatest concentrations of microcharcoal were recorded (from 23 – 22 cal ka BP). There is a small peak in Juncaceae percentages at the base of the sequence and peaks in Cyperaceae around 22 cal ka BP, although wetland taxa percentages are generally somewhat reduced for PB1-A.

For PB-1B (21 - 14.5 cal ka BP) we observe significantly elevated percentages of Restionaceae within the sand layer dating to ~20 - 15.5 cal ka BP (Fig. 4 and Fig. 5), coinciding with generally reduced succulent/drought-resistant taxa and fynbos elements relative to PB1-A. The highest peak in the aquatic taxon Haloragaceae for the sequence (12%) and peaks in the coastal thicket taxa *Canthium* and *Morella* also characterise PB1-B. While *Dodonaea* reappears near the top of PB1-B, this taxon is recorded in more significant proportions within PB1-C (14.5 - 12 cal ka BP), together with relatively elevated percentages in other coastal thicket indicators (e.g. *Canthium* and *Morella*) and the afrotemperate forest taxon *Clutia*. Fynbos (Ericaceae, Restionaceae, Proteaceae and *Stoebe*-type) proportions remain relatively high for this period. The succulent/drought-resistant taxa *Crassula*, *Euphorbia* and *Ruschia* all exhibit prominent peaks within this PB1-C.

Pollen was not found in sediments dating to the early Holocene (11.7 – 8 cal ka BP). For most of the mid- to late Holocene (PB1-D; ~7.7 - 0 cal ka BP), other than Restionaceae which remains relatively high, fynbos elements (particularly Ericaceae and *Passerina*) are represented in much lower proportions in comparison to the previous zones. The halophytic taxon Amaranthaceae peaks from 6 - 5 cal ka BP and is generally represented in high proportions within the whole of PB1-D. Coinciding with the peak in Amaranthaceae are peaks in *Ruschia*, *Crassula* and microcharcoal concentrations. Microcharcoal concentrations and amounts (for both size classes) peak again from 2 - 1 cal ka BP. Asteraceae percentages are generally higher within PB1-D compared to the previous zones and reach a maximum for the sequence

(38%) at ~4.2 cal ka BP. Wetland taxa generally exhibit no clear trends/changes other than a small peak in Blechnaceae at base of the zone, at ~7.7 cal ka BP and peaks in Cyperaceae at ~5.8 and ~1.9 cal ka BP.

The most recent portion of the record, the last 500 years (PB1-D3), is substantially different from the rest of the Holocene section, being characterised by exceptionally high percentages of Proteaceae (up to 26%), distinct peaks in *Cliffortia*, Amaranthaceae, *Euclea*, *Morella* and *Dodonaea*, and the appearance of *Sideroxylon* pollen.

DISCUSSION

The pollen results from the Pearly Beach sediment core reveal that distinct changes in vegetation composition occurred along the southwestern Cape coast since the onset of the LGM. The analysis of contemporary climatic constraints on the identified taxa (Figs. 6 and 7) provides a framework for the interpretation of this record. Considerable variability in temperature and moisture availability may be inferred from these results, which are of particular importance in shedding new light on the LGM and Termination I in the region. The Holocene portion of the record is of significantly lower resolution, but it provides important context for understanding the climate and vegetation history of the site. As the site is located 2.5 km from the modern coastline, and ~28.5 km from the LGM coastline (Spratt and Lisiecki, 2016; Group, 2020), the potential impact of changing sea-level should be considered when considering the Pearly Beach data. The gradient of the adjacent shelf is low and regular, and the coastline is predicted to have encroached upon the site at a rate of ~1.6 km/ka since the LGM, achieving its current position at ~5 ka. Considering the position and palaeo-landscape of the site, factors such as increased continentality are unlikely to have been a significant factor, and a related progressive increase in moisture availability with reduced distance to the coast is not indicated by the pollen record, as will be described (Fig. 5). Similarly, rising sea-levels would have raised base-level and associated groundwater levels, but again the records do not indicate an increase in water-availability with a rise in base-level. Sea-level changes and

the position of the site relative to the coast may also have had an impact on sedimentation regimes, with marine transgression resulting in an increase in marine and aeolian sands. Grain size results from the sediment core (Fig 4.), however, indicate no pattern that can be readily associated with sea-level change, such as an increase in the coarse sediment fraction. Thus, in the absence of specific evidence for a strong marine impact, the record is presently interpreted primarily in terms of climate.

The Last Glacial Maximum (LGM; ~25.3-19 cal ka BP)

Pollen from cold-tolerant fynbos taxa (*e.g. Stoebe*-type, *Passerina* and Ericaceae) indicate that these plants were dominant features of the Pearly Beach landscape from 25.3 – 22.5 cal ka BP (Figs. 5, 6 and 7). This is consistent with other evidence of cooler conditions throughout southern Africa during the last glacial period and LGM in particular (Heaton et al., 1986; Talma and Vogel, 1992; Stute and Talma, 1998; Truc et al., 2013; Chevalier and Chase, 2015). However, the presence of *Dodonaea* pollen, a relatively frost intolerant taxon (Valsecchi et al., 2013) (Fig. 6), suggests that frost — if it occurred — was not common.

During this period, the coastal thicket group is dominated by a relatively high abundance of *Euclea* and Santalaceae pollen (likely *Thesium*, based on associations with increased fynbos representation at this time), which, coupled with the co-occurrence of *Ruschia* pollen, may reflect a relatively xeric coastal thicket composition (Boucher and Moll, 1981; Boucher, 1987; Cowling et al., 1999). While more mesic taxa such as *Morella*, *Canthium*, and the afrotemperate taxa *Podocarpus/Afrocarpus* and *Myrsine* are present, they are found only in relatively low proportions (Figs. 5, 6 and 7). Cooler conditions at this time thus do not seem to be associated with either a significant decline in moisture availability (as has been inferred from charcoal data from Boomplaas Cave (Deacon et al., 1984; Scholtz, 1986)). Nor however do they seem to reflect substantially wetter conditions during the LGM, as indicated in some palaeoclimate model simulations (Engelbrecht et al., 2019), and has been inferred from evidence elsewhere in the WRZ, such as Elands Bay Cave (Cartwright and Parkington, 1997; Cowling et al., 1999; Parkington et al., 2000).

366 Considered in the context of the record as a whole, *Euclea* does exhibit a general positive relationship
367 with microcharcoal concentrations (Fig. 5), suggesting that fire may also be a factor contributing to the
368 dominance of *Euclea* in the coastal thicket at this time. *Euclea* (e.g. *E. racemosa*) may have been able to
369 exert a competitive advantage over more mesic, less fire-adapted thicket taxa under a regime of more
370 regular fire occurrence (Nzunda and Lawes, 2011).

371 The period from ~22.5-22 cal ka BP is characterised by high levels of succulent/drought-resistant
372 pollen and decreased levels of both coastal thicket and afrotemperate forest taxa, indicating a period of
373 relatively dry conditions (Fig. 5 and Fig. 8). High percentages of *Stoebe*-type pollen suggest this interval
374 was also perhaps the coolest of the last 25 kyr. At ~22 cal ka BP, this phase of cool and relatively dry
375 conditions is disrupted abruptly by an episode of increased temperatures and humidity, as indicated by
376 strong increases in *Morella* and *Dodonaea* pollen (Fig. 5 and Fig. 6). While brief, the timing of this event is
377 consistent with episodes of increased humidity in other regional records, at Seweweekspoort (Chase et
378 al., 2017) and along the southwest African margin (Chase et al., 2019b).

379 The late LGM, from ~22-19 cal ka BP, is characterised by a further decline in coastal thicket and
380 afrotemperate forest taxa and a dominance of Restionaceae pollen in association with greater
381 contributions of medium and coarse-grained sands (Figs. 4 and 5). These trends may reflect the ceding of
382 the thicket niche to Restionaceae species that are more tolerant of summer drought (e.g. *Thamnochortus*,
383 which is common on dunes along the arid, winter-rain dominated west coast (Linder and Mann, 1998;
384 SANBI, 2003)). The thicket taxa *Morella* and *Canthium* begin to become more prominent at ~20 cal ka BP,
385 suggesting the beginning of an increase in humidity that accelerates rapidly (reflected in substantial
386 increases in these taxa) with the onset of Southern Hemisphere warming at ~19 ka.

387 In terms of drivers of the patterns of vegetation change observed in the Pearly Beach pollen record,
388 the data are consistent with indications from elsewhere in southwestern Africa (e.g. Chase et al., 2015a;

389 Chase et al., 2019b) that AMOC was a strong modulator of global LGM conditions. At Pearly Beach,
390 changes in the pollen record – while complex – are in accord with results from Namib Desert rock hyrax
391 middens, which indicate phases of relatively drier conditions (~24-22.5 cal ka BP and ~22-18 cal ka BP)
392 demarcated by brief phases of increased humidity from ~24.5-24 cal ka BP and 22.5-22 cal ka BP prior to
393 the beginning of Termination I (Chase et al., 2019b) (Fig. 9).

394 At variance with the inference that the cool/cold boundary conditions of the terminal Pleistocene
395 created relatively humid conditions in the southwestern Cape (van Zinderen Bakker, 1976; Cockcroft et
396 al., 1987; Cowling et al., 1999), the Pearly Beach record suggests that phases of increased humidity
397 correlate positively with increased temperature (Figs. 9 and 8). This likely relates to a combination of
398 factors linked to a progressive build-up of heat in the South Atlantic and high southern latitudes associated
399 with weaker AMOC (Stocker and Johnsen, 2003; McManus et al., 2004; Ng et al., 2018). This warming -
400 including the Southeast Atlantic and oceans surrounding the southwestern Cape (Kim et al., 2003; Farmer
401 et al., 2005; Dyez et al., 2014) - may have influenced regional climates through: 1) a southerly shift of the
402 Atlantic Intertropical Convergence Zone (ITCZ) and African rainbelt (Broccoli et al., 2006), including a
403 weakening of the SE Trade Winds and a southerly shift of the Angola-Benguela Front (Kim et al., 2003)
404 (Fig. 1), 2) a poleward displacement of the Subtropical Front and westerlies storm track (Lee et al., 2011;
405 Menviel et al., 2018) (likely also enabling increased Agulhas leakage into the SE Atlantic (Peeters et al.,
406 2004; Caley et al., 2012)), but a warming of the Southwest Atlantic and waters upstream from the
407 southwestern Cape, increasing moisture uptake by the frontal systems that bring winter rains to the Cape
408 (Reason et al., 2002; Reason et al., 2006), and 3) increased evaporation and advection of moisture from
409 southern coastal waters, fostering the development of localised precipitation systems (Jury et al., 1993;
410 Jury et al., 1997). All of these factors could result in a less seasonal rainfall regime and a shorter/less
411 intense drought season in the southwestern Cape (Chase et al., 2015b). At the subcontinental scale, it has
412 been observed that warm events in the Southeast Atlantic off Angola and Namibia are associated with

increased rainfall along southern Africa's western margin, and that these anomalies may extend inland significantly, particularly if easterly flow off the Indian Ocean is also high (Rouault et al., 2003). A critical dynamic may have thus been fostered between the warming and southward displacement of the Angola-Benguela Front (Fig. 1) and the increased moisture uptake of westerly frontal systems.

Today, cloud bands known as tropical-temperate troughs (TTTs) account for a significant proportion of southern Africa's summer rainfall and are a major mechanism for the poleward transfer of energy (Todd and Washington, 1999). The potential of TTTs and other forms of tropical temperate interactions (TTIs) to have been an important factor in determining synoptic-scale climate dynamics in southern Africa during the last glacial period has been highlighted, and considered to be a possible explanation for similarities in patterns of climate change across the continental interior (Chase, 2010; Chase et al., 2017). These types of synoptic systems have been identified as having an important influence on modern southern Cape climates (Engelbrecht et al., 2015), and similarities evident between the Pearly Beach record and records of climate change from sites in the Namib Desert (Chase et al., 2019b) (Fig. 9) suggest that the interactions between tropical and temperate regions may have been enhanced during periods of elevated southeast Atlantic SSTs, and associated cloud bands and other related disturbances may have formed further to the southwest than is common today.

Termination I (~19-11.7 cal ka BP)

At Pearly Beach, the onset of Southern Hemisphere warming and the end of the LGM is associated with more abundant moisture, as indicated by the development of coastal thicket vegetation and a reduction in succulent/drought resistant pollen from ~19 – 13 cal ka BP (Figs. 5 and 8). In contrast to the thicket composition of the early LGM, *Canthium* is the dominant taxon at ~18.4 cal ka BP (Fig. 5). *Canthium* is most prevalent in humid coastal regions from the Knysna region eastward (SANBI, 2003), and at Pearly Beach it is a clear indicator of warmer, moister conditions (Fig. 7), likely implying significant contributions

436 of summer rainfall as a result of the climate system dynamics described above. Interestingly, *Canthium*
437 quickly cedes dominance to *Morella*, which establishes itself as the most prominent thicket taxon for the
438 period 18-14.5 cal ka BP, broadly coincident with the Heinrich stadial 1 chronozone (HS1; ~18.5-14.6 cal
439 ka BP).

440 *Morella* and *Canthium* occupy very similar climatic niches, and the progression from *Canthium* to
441 *Morella* dominance in the thicket taxa pollen spectrum may have been due to non-climatic mechanisms
442 related to vegetation succession, as has been noted at other southern Cape sites (cf. Quick et al. 2016).
443 *Morella* species likely do occur at the site (e.g. *M. quercifolia*) and are associated with stabilised sand
444 dunes. *Canthium inerme* and *Afrocanthium mundianum* are associated with coastal forests and dune
445 thicket but may have a closer association to active stream networks than *Morella*. The landscape
446 surrounding Pearly Beach, comprises a low relief coastal platform (<30 m.a.s.l.) occupied by alluvial and
447 aeolian sediments – including an extensive semi-active to primarily dormant dunefield – and a significant
448 stream network associated with upland catchments to the north and northeast. The landscape dynamics
449 of the immediate region therefore have potential to create a complex and changing mosaic of ecological
450 niches. Therein, the observation that peaks in *Canthium* effectively bracket phases of *Morella* dominance
451 may be associated with differences in the response time between fluvial systems and dunefields to
452 changes in rainfall. While dune stabilisation under more humid conditions may be a protracted process,
453 increased rainfall would have a much more immediate impact on fluvial activity and the development of
454 riparian zones, thus potentially favouring the early establishment of *Canthium* over *Morella*. Once the
455 dunefields became more stable, *Morella* would have become more prevalent. Conversely, increased
456 aridity may have a more immediate impact on dunefield vegetation, as fluvial networks may continue to
457 be fed by rainfall in the adjacent uplands and through groundwater discharge, maintaining higher levels
458 of water availability at seeps and along channels.

Regardless of successional or landscape/hydrologic dynamics, the marked increase in *Canthium* and *Morella* pollen – and indeed coastal thicket taxa as a group – at ~18.5 cal ka BP indicating a substantial increase in moisture availability, is coincident, and perhaps associated with slowing AMOC (McManus et al., 2004; Ng et al., 2018) and a build-up of heat in the southern Atlantic (Fig. 9). As has been noted elsewhere (Chase et al., 2015a; Chase et al., 2019b), the response in terrestrial environments in southwestern Africa to changes in AMOC associated with HS1 is not predicted to be immediate. The rapid slow-down in AMOC at the beginning of HS1 resulted in a relatively slow, progressive build-up of heat in the South Atlantic and high southern latitudes, which culminates in maximum temperatures being reached at the very end of HS1, at ~14.6 cal ka BP (Kim and Schneider, 2003; Farmer et al., 2005; Jouzel et al., 2007; Pedro et al., 2011)(Fig. 9). As has been described for the LGM, these changes in SSTs in the Southeast Atlantic and oceans surrounding the southwestern Cape may have resulted in a less seasonal rainfall regime. At such times increased summer rainfall may have been derived from both localised precipitation systems (Jury et al., 1993; Jury et al., 1997) and the development of the aforementioned larger synoptic scale TTTs /TTIs (Todd and Washington, 1999), which may have been more prevalent in the region given elevated west coast SSTs (Fig. 9). At Pearly Beach these changes are reflected by high coastal thicket taxa pollen percentages and a strong increase in *Dodonaea* pollen (Fig. 5), indicating warm, humid conditions under a less seasonal rainfall regime.

Similarities with the deglacial record from Pearly Beach are observed across a wide range of terrestrial records not only from the southern and southwestern Cape (Chase et al., 2015a; Quick et al., 2016) and the western margin of southern Africa (Chase et al., 2015a; Lim et al., 2016; Chase et al., 2019b) – regions under the immediate influence of the South Atlantic anticyclone and the westerlies – but also from the ARZ (Scholtz, 1986; Chase et al., 2017) and the SRZ (Chevalier and Chase, 2015), emphasising the subcontinental-scale influence of the slow-down of AMOC during HS1 (Fig. 9).

HS1 ended at 14.6 ka, and at Pearly Beach this transition is marked by variable, declining levels of coastal thicket pollen and increases in pollen from xeric taxa such as *Ruschia* (Fig. 5). Coupled with increases in pollen from plants favouring cool/cold conditions — such as *Stoebe*-type and Ericaceae between ~13.9-12.6 cal kBP, the evidence seems to suggest that the increased AMOC strength (Ng et al., 2018) that triggered cooling in the southeast Atlantic (Kim and Schneider, 2003; Farmer et al., 2005) and the high southern latitudes (e.g. Jouzel et al., 2007) – the Antarctic Cold Reversal (Pedro et al., 2016) – resulted in relatively cool, dry conditions at Pearly Beach (Fig. 9). The subsequent Younger Dryas period is characterised by slight increases in pollen from both cool/cold and coastal thicket taxa, perhaps indicating a modest increase in winter rainfall. As has been noted elsewhere (Chase et al., 2015a), the magnitude of forcing associated with the Younger Dryas was substantially less than it was for HS1, and left an accordingly less distinct signature in most southwestern Africa records, with greater spatial heterogeneity.

The Holocene (7.8 – 0.3 cal ka BP)

No pollen was preserved in the sediments dating to ~12-7.8 cal ka BP in the Pearly Beach core. It could be speculated that the limited preservation of pollen within the Pearly Beach core during the early Holocene was a response to increased aridity, as inferred from micromammalian data from Byneskranskop, an archaeological site 8 km northwest of Pearly Beach (Faith et al., 2018, 2020; Thackeray, 2020). Indications of relatively low moisture availability are also evident from further east within the Wilderness embayment (Martin, 1968; Quick et al., 2018), and the summer-rainfall zone (e.g. Holmgren et al., 2003), related, in part, to increased drought stress under warmer Holocene temperatures (Chevalier and Chase, 2016).

The resolution of the Holocene record allows for the identification of multi-millennial trends, but it lacks the detail required to make definitive inferences regarding the primary mechanisms driving climate change. As a whole, coastal thicket pollen percentages are relatively low until the recent past, when a strong increase is observed at ~ 0.3 cal ka BP. This suggests generally drier Holocene conditions compared

505 to the Late Pleistocene, with a modest, but notable increase in apparent humidity in the mid-Holocene,
506 from ~6-4 cal ka BP (Figs. 5 and 9).

507 The recovery of high resolution records from the southwestern Cape, from Katbakkies Pass (Chase
508 et al., 2015b) and Pakhuis Pass (Chase et al., 2019a) have enabled correlations with records for Southern
509 Ocean SSTs and sea-ice extent (Nielsen et al., 2004) during the Holocene. These have been interpreted to
510 indicate a phase of increased westerly influence during the mid-Holocene, which may account for the
511 increased humidity at Pearly Beach. However, when considered in the context of other comparable
512 records from the region, a pattern of marked spatial heterogeneity is observed (Chase et al., 2015a; Chase
513 et al., 2019a), particularly between coastal and interior sites (Chase and Quick, 2018; Quick et al., 2018).
514 Furthermore, the mid-Holocene in the Cape is a period of significant climatic variability, and while efforts
515 have been made to establish diagnostic patterns of change that can be used to infer specific drivers (Chase
516 et al., 2017; Chase and Quick, 2018; Chase et al., 2020), the Pearly Beach record currently lacks the
517 requisite resolution to draw meaningful conclusions in this regard. What is evident, is that at Pearly Beach
518 there are significant changes in the overall vegetation composition between the deglacial and Holocene,
519 with a clear shift from ericaceous fynbos in the late Pleistocene to other structural types of fynbos
520 (proteoid, restioid and asteraceous) in the middle and late Holocene. These changes are likely in response
521 to increased Holocene temperatures and relatively drier conditions as compared to HS1 and at least some
522 phases of the LGM.

523 The last 500 years is characterised by a significant increase in coastal thicket (e.g. *Euclea, Morella*
524 and *Sideroxylon,* as well as *Dodonaea*, comparable to the peaks during HS1) and represents the
525 culmination of the steady rise in Proteaceae percentages across the Holocene (Fig. 5). While the above
526 mentioned taxa suggest more humid conditions, consistent with coeval increases in temperature and
527 humidity as indicated by the record as a whole, there is also an increase in Amaranthaceae and *Ruschia*

pollen, suggesting at least some phases of more arid conditions, and probably an increase in climate variability. The sharp increase in thicket taxa in the sample dated to ~0.3 cal ka BP is consistent with marked changes in inferred water availability in higher resolution records from Bo Langvlei (du Plessis et al., 2020), Seweweekspoort (Chase et al., 2017) and the Namib region (Chase et al., 2019b). Again, however, the resolution of this portion of the Pearly Beach record – in terms of both pollen and radiocarbon samples – does not allow for a clearer attribution of this increase in thicket pollen to either an increase in summer rainfall following the Little Ice Age (0.1-0.7 cal ka BP), as speculated at Bo Langvlei (du Plessis et al., 2020), or an increase in winter rainfall during the LIA, as inferred from diatom data at Verlorenvlei, on the west coast (Stager et al., 2012).

CONCLUSIONS

In this paper we present new fossil pollen, microcharcoal and sediment particle size data from a 25,000-year sediment core taken from a wetland at Pearly Beach, southwestern Cape coast of South Africa. The results reveal considerable variability in vegetation composition and by inference climate - along the southwestern Cape coast since the onset of the LGM. We find that the Pearly Beach record is generally consistent with indications from elsewhere in southwestern Africa (Chase et al., 2015a; Lim et al., 2016; Chase et al., 2019b) that AMOC through its impact on regional oceanic and atmospheric circulation systems was potentially a strong modulator of global LGM boundary conditions, resulting in phases of relatively drier conditions (~24-22.5 cal ka BP and ~22-18 cal ka BP) demarcated by brief phases of increased humidity from ~24.5-24 cal ka BP and 22.5-22 cal ka BP. During Termination I, the marked increase in coastal thicket pollen at ~18.5 cal ka BP indicates a substantial increase in moisture availability, coincident, and likely associated with slowing AMOC and a build-up of heat in the southern Atlantic during HS1. The resolution of the Holocene portion of the record does not allow for definitive inferences regarding the primary mechanisms driving climate change, but it is evident that there are significant

changes in the overall vegetation composition between the deglacial and Holocene, with a clear shift from ericaceous fynbos in the late Pleistocene to other structural types of fynbos (proteoid, restioid and asteraceous) in the middle and late Holocene. These changes are likely in response to increased Holocene temperatures and relatively drier conditions.

Overall, the Pearly Beach record represents an important new contribution to a growing body of data that provides evidence for great spatial complexity in regional climatic responses, and more specifically, provides evidence that AMOC variability influence extended eastwards along the southwestern Cape coast at least as far as the modern boundary of the WRZ. It also provides a rare look at the response of lowland sectors of the mega-diverse Cape Floristic Region to major long-term climatic transitions.

Data Availability

The full pollen, charcoal and particle size datasets are given in Appendix A (Supplementary data) and will also be available on the Neotoma Palaeoecology data archive (https://www.neotomadb.org/) as a contribution to the African Pollen Database.

Acknowledgements

L.J.Q. acknowledges the financial assistance of the National Research Foundation (NRF) of South Africa, PAST (Palaeontological Scientific Trust) and the University of Cape Town. This study was funded in part by the European Research Council (ERC) under the European Union's Seventh Framework Programme (FP7/2007-2013)/ERC Starting Grant "HYRAX", grant agreement no. 258657. We thank Carmen Kirchner for conducting the particle size analysis at the Department of Geography, Friedrich-Schiller-University, Jena. We also thank Rachid Cheddadi and Graciela Gil-Romera for assisting with recovery of the core.

Figures and figure captions

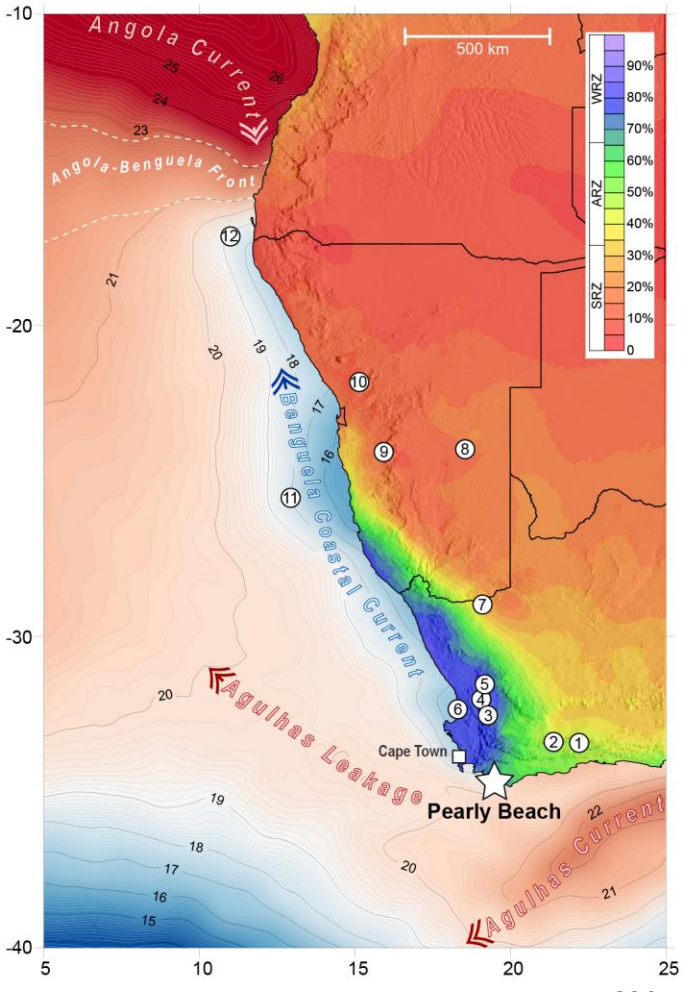

Figure 1. Map of the southwestern margin of Africa showing seasonality of rainfall and sharp climatic gradients dictated by the zones of summer/tropical (red) and winter/temperate (blue) rainfall dominance. The major oceanic circulation systems (the cold Benguela current and the warm Agulhas and Angola currents, temperatures shown in °C (Reynolds et al., 2007)) are indicated as well as the position of Pearly Beach (star) in relation to key palaeoclimatic records (1 – Cango Caves (Talma and Vogel, 1992), 2 – Seweweekspoort (Chase et al., 2013; Chase et al., 2017), 3- Katbakkies Pass (Meadows et al., 2010; Chase et al., 2015b), 4 – De Rif (Chase et al., 2011; Quick et al., 2011; Valsecchi et al., 2013; Chase et al., 2015a), 5 – Pakhuis Pass (Scott and Woodborne, 2007c, a; Chase et al., 2019a), 6 – Elands Bay Cave (Cowling et al., 1999; Parkington et al., 2000), 7 – Pella (Lim et al., 2016; Chase et al., 2019b), 8 – Stampriet Aquifer (Stute and Talma, 1998), 9 – Zizou (Chase et al., 2019b), 10 – Spitzkoppe (Chase et al., 2009; Chase et al., 2019b), 11 – ODP 1084B (Farmer et al., 2005), 12 – GeoB 1023-5 (Kim et al., 2003).

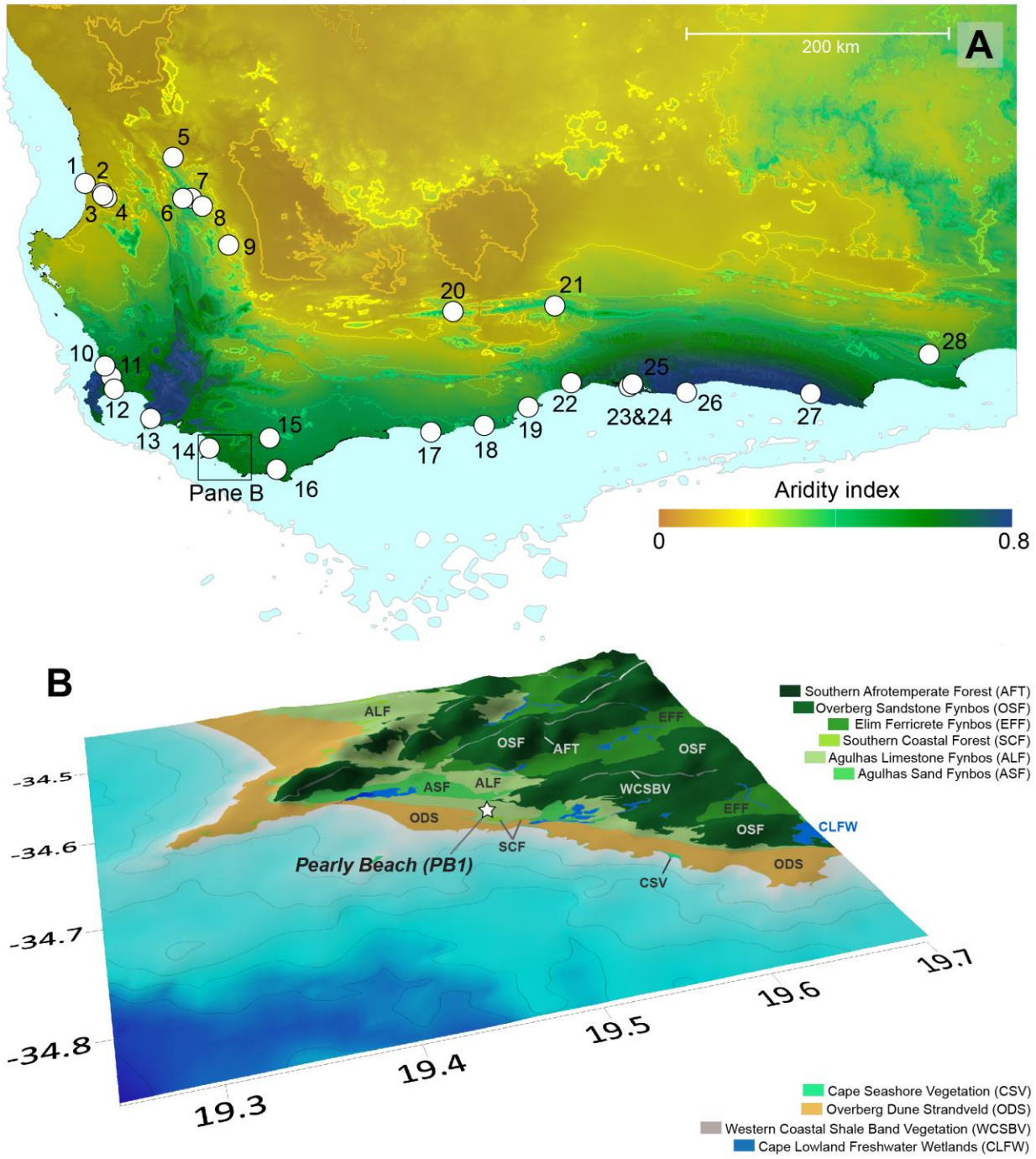

Figure 2. Pane A: Aridity index map of the southwestern Cape (data: Zomer et al., 2008) , with lower values indicating drier conditions. Peripheral blue shading indicates position of shoreline at Last Glacial Maximum low-stand (-130 m). The locations of published palaeoenvironmental and archaeological records from the region are shown: 1 – Elands Bay Cave (Parkington et al., 1988; Cowling et al., 1999; Parkington et al., 2000), 2 – Grootdrift (Meadows et al., 1996), 3 – Verlorenvlei (Kirsten et al.; Stager et al., 2012; Carr et al., 2015), 4 – Klaarfontein Springs (Meadows and Baxter, 2001), 5 – Pakhuis Pass (Scott and Woodborne,

2007b, c), 6 – Sneeuberg Vlei and Driehoek Vlei (Meadows and Sugden, 1991), 7 – De Rif (Chase et al., 2011; Quick et al., 2011; Valsecchi et al., 2013; Chase et al., 2015a), 8 – Truitjes Kraal (Meadows et al., 2010), 9 Katbakkies (Meadows et al., 2010; Chase et al., 2015b), 10 Rietvlei (Schalke, 1973), 11 – Cape Flats (Schalke, 1973), 12 – Princess Vlei (Neumann et al., 2011; Kirsten and Meadows, 2016; Cordova et al., 2019), 13 – Cape Hangklip (Schalke, 1973), 14 – Die Kelders (Klein and Cruz-Uribe, 2000), 15 – Bynekranskop (Schweitzer and Wilson, 1982; Faith et al., 2018), 16 – The Agulhas Plain vleis and lunettes (Soetendalsvlei, Voëlvlei, Renosterkop and Soutpan) (Carr et al., 2006a; Carr et al., 2006b), 17 – Blombos Cave (Henshilwood et al., 2001), 18 – Rietvlei-Still Bay (Quick et al., 2015), 19 – Pinnacle Point (Marean, 2010; Rector and Reed, 2010), 20 – Seweweekspoort (Chase et al., 2013; Chase et al., 2017), 21 – Cango Cave (Talma and Vogel, 1992) and Boomplaas Cave (Deacon et al., 1984), 22 – Norga peats (Scholtz, 1986), 23 – Eilandvlei (Kirsten et al., 2018; Quick et al., 2018; Wündsch et al., 2018) and Bo Langvlei (du Plessis et al., 2020), 24 – Groenvlei (Martin, 1968; Wündsch et al., 2016), 25 – Vankervelsvlei (Irving and Meadows, 1997; Quick et al., 2016), 26 – Nelson Bay Cave (Cohen and Tyson, 1995), 27 – Klasies River Mouth (Deacon et al., 1986) and 28 Uitenhage Aquifer (Heaton et al., 1986; Stute and Talma, 1998).

Pane B: Location of Pearly Beach 1 sediment coring site in relation to the current distribution of dominant vegetation types [Data: South African National Biodiversity Institute (2006-). The Vegetation Map of South Africa, Lesotho and Swaziland, Mucina, L., Rutherford, M.C. and Powrie, L.W. (Editors), Online, http://bgis.sanbi.org/SpatialDataset/Detail/18, Version 2018]. Bathymetry contours are at 20 m intervals (GEBCO, 2012) and 0.1° grid intervals equate to ~9.2 km at this latitude.

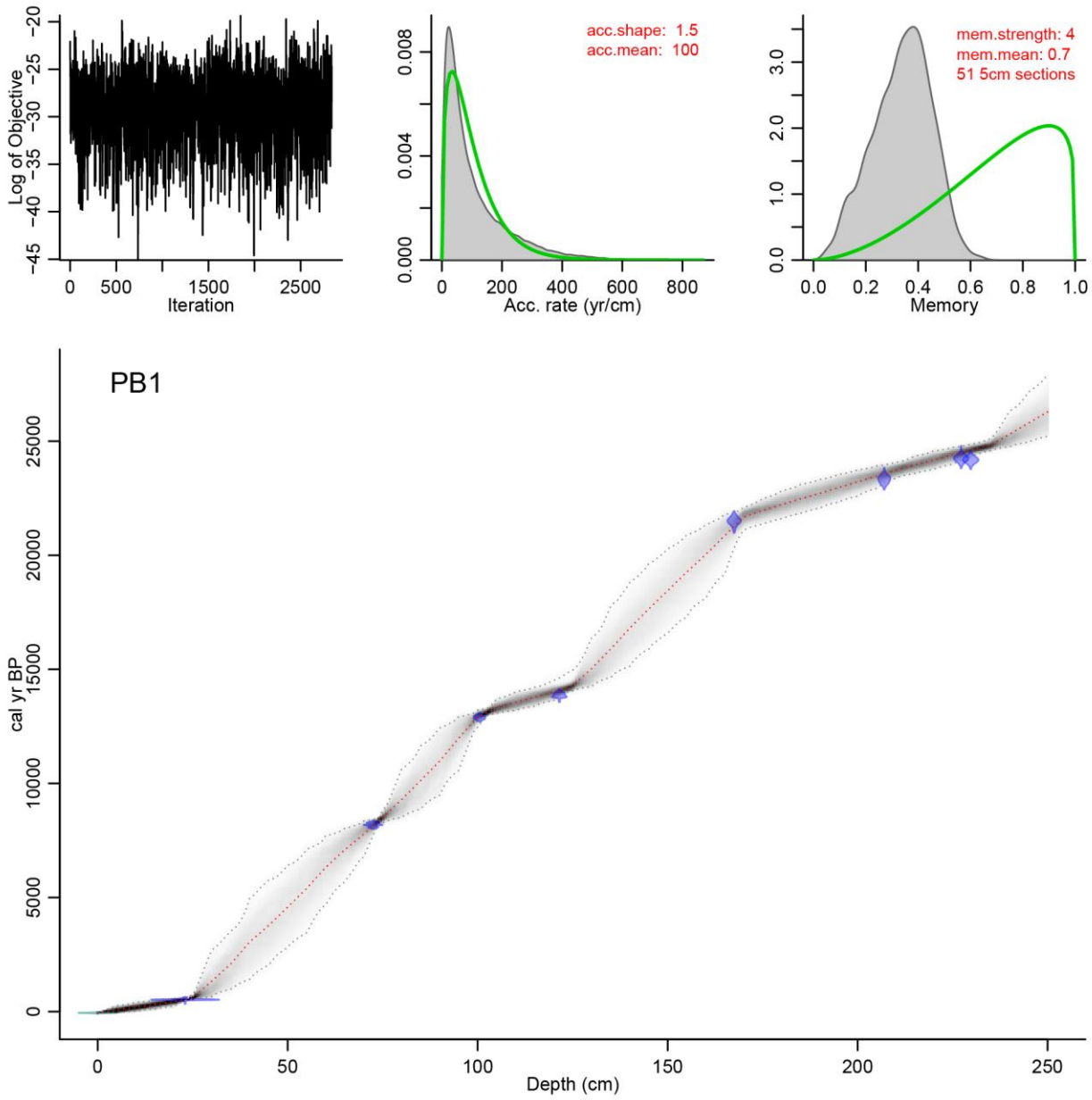

622

623 Figure 3. Age-depth model for Pearly Beach (PB1) using the *Bacon* software package (Blaauw and Christen,
624 2011). The blue areas represent the 2σ probability distributions of the calibrated ^{14}C ages, the grey-scales
625 indicate all likely age-depth models, grey dotted lines show the 95% confidence intervals and the red
626 dotted line shows the single 'best' model based on the median age for each depth.

627

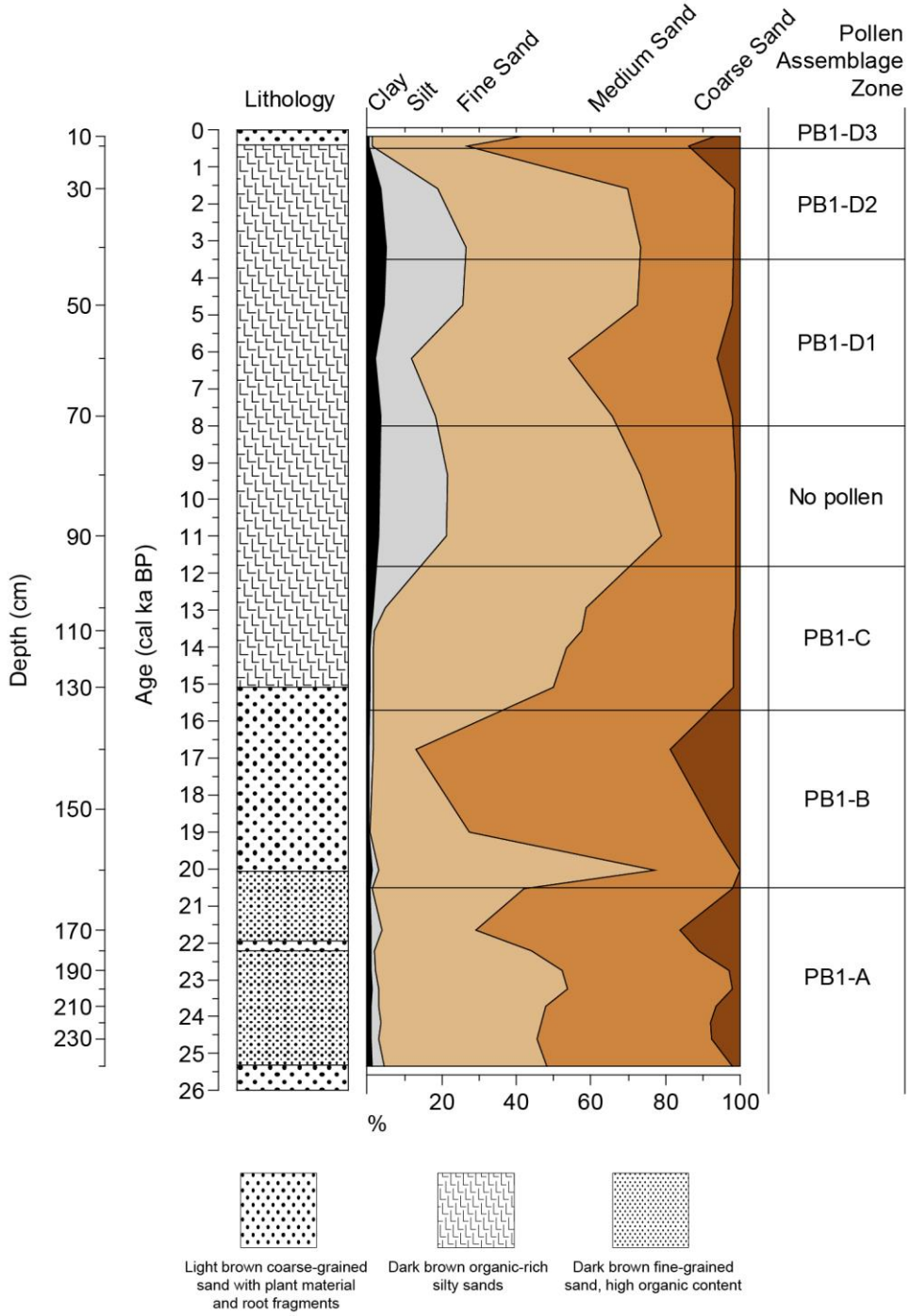

628

629 Figure 4: Pearly Beach 1 (PB1) particle size analysis data displayed as percentages of clay (0 – 2 µm), silt
630 (2 – 20 µm), fine sand (20 – 200 µm), medium sand (200 – 500 µm) and coarse sand (500 – 2000 µm)
631 plotted against interpolated age (cal kBP) and composite depth (cm) with pollen assemblage zones
632 indicated on the far right.

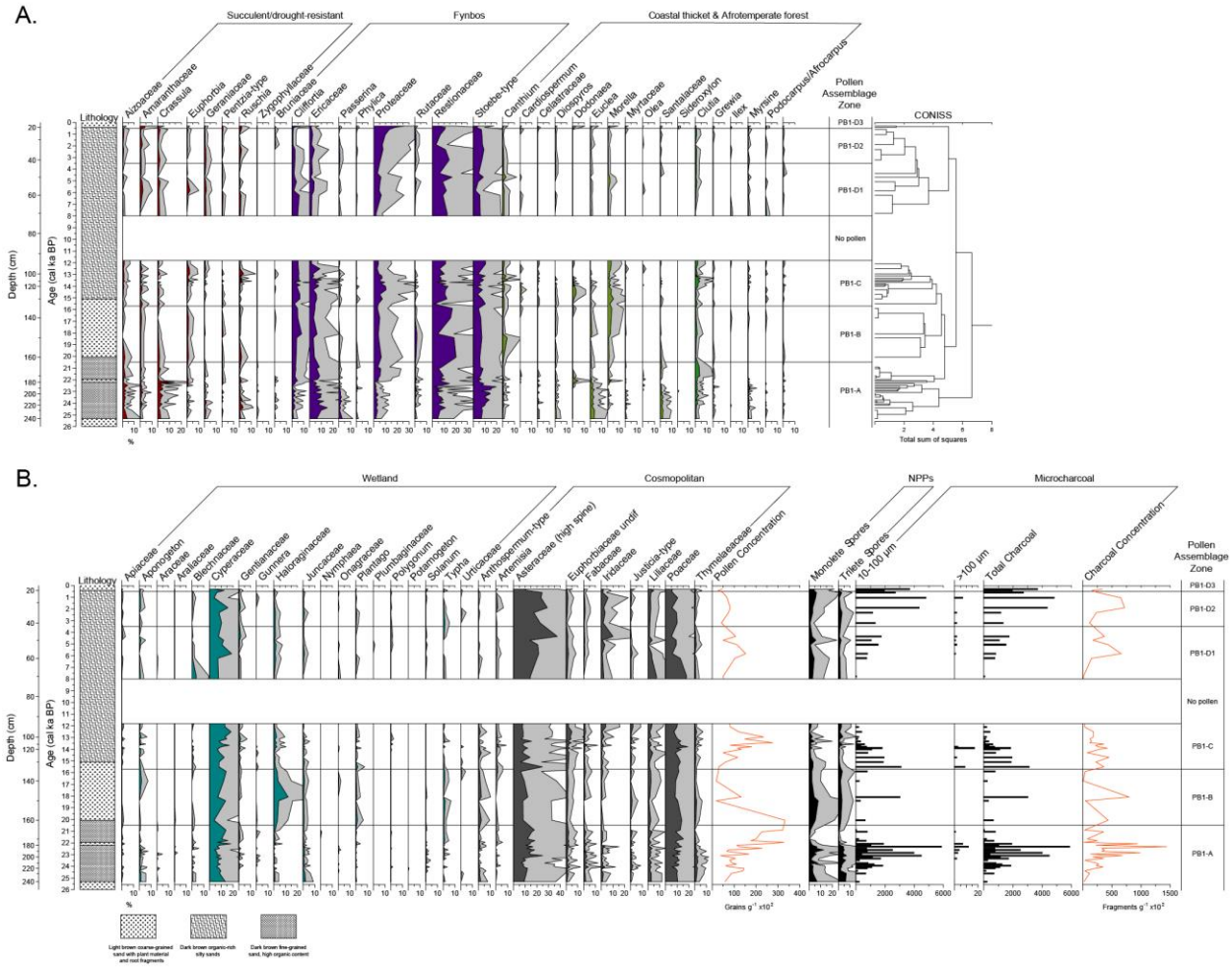

633

634 Figure 5 (A and B): Relative percentage pollen and microcharcoal diagrams for Pearly Beach (PB1). Taxa
635 grouped according to general ecological affinities and are plotted against interpolated age (cal kBP) and
636 composite depth (cm). Taxa included in the Cosmopolitan ecological grouping that represent less than 2%
637 for any given level were excluded, the full dataset is presented in Appendix A. Exaggeration curves are 3x
638 and zonation is based on the results of a CONISS analysis.

639

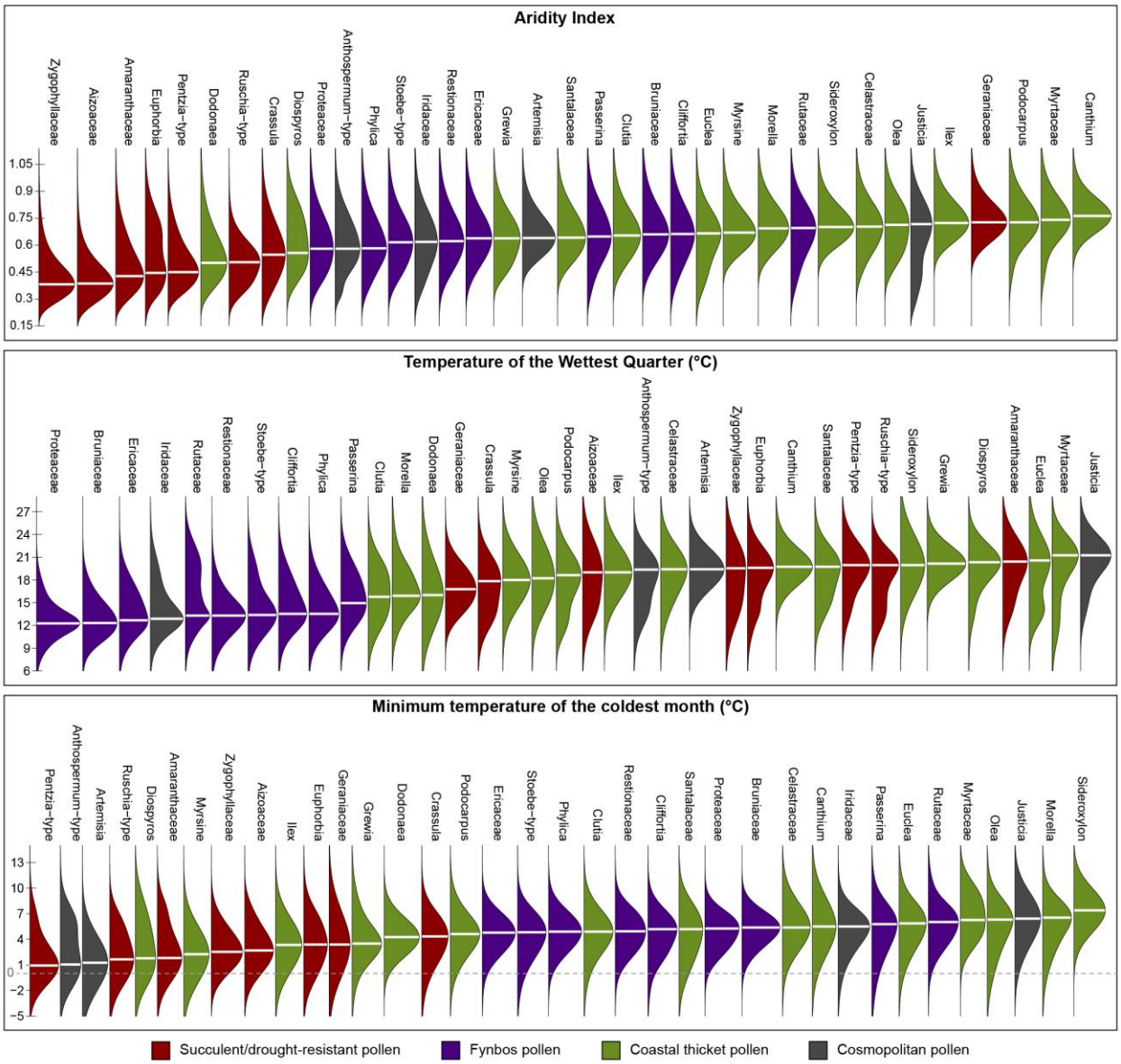

Figure 6: Probabilistic responses of the pollen taxa to three important regional climate determinants: Aridity index (Zomer et al., 2008; Trabucco and Zomer, 2019) and the temperature of the wettest quarter (used as a proxy for the temperature of the growing season) and the minimum temperature of the coldest month (Fick and Hijmans, 2017). These responses were calculated following the probability density function (pdf) approach of Chevalier et al. (2014) and using data from the SANBI database (SANBI, 2003), restricted to the plant species that currently live in the study area (defined here as a box between 17° and 29°E and between 32° and 35°S).

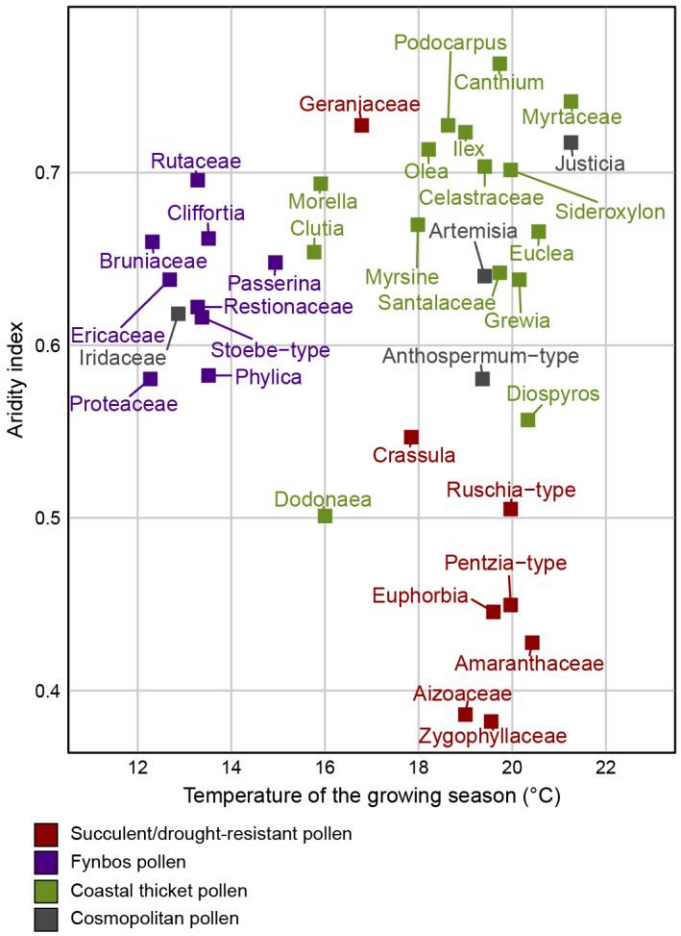

Figure 7: Biplot representing the climate optima (*i.e.* the climate value with the highest probability of presence) of the studied taxa for the temperature of the growing season (x-axis) (as represented by temperature of the wettest quarter) and aridity (y-axis; larger values associated with more humid conditions).

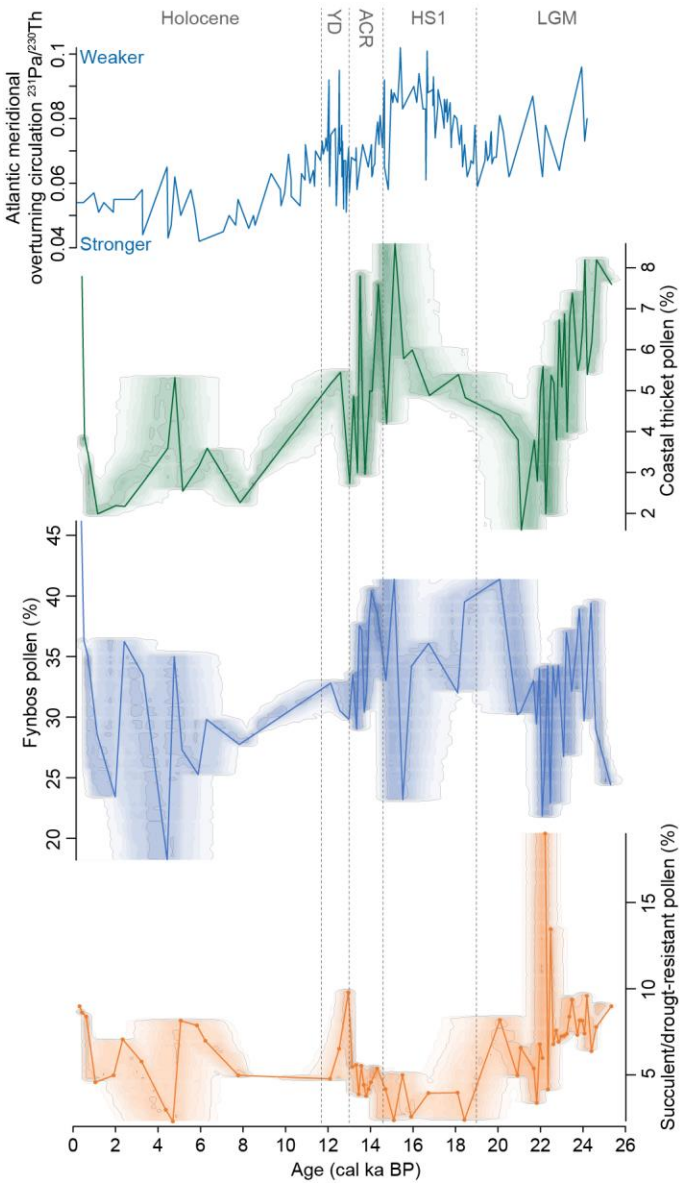

Figure 8: Primary pollen groups from Pearly Beach (PB1). Associated shading was obtained from proxy ghost analysis using *rbacon* software (v. 2.3.6; Blaauw and Christen, 2011) to express chronological uncertainties. The Holocene, Younger Dryas (YD), Antarctic Cold Reversal (ACR) and Last Glacial Maximum (LGM) chronozones are indicated.

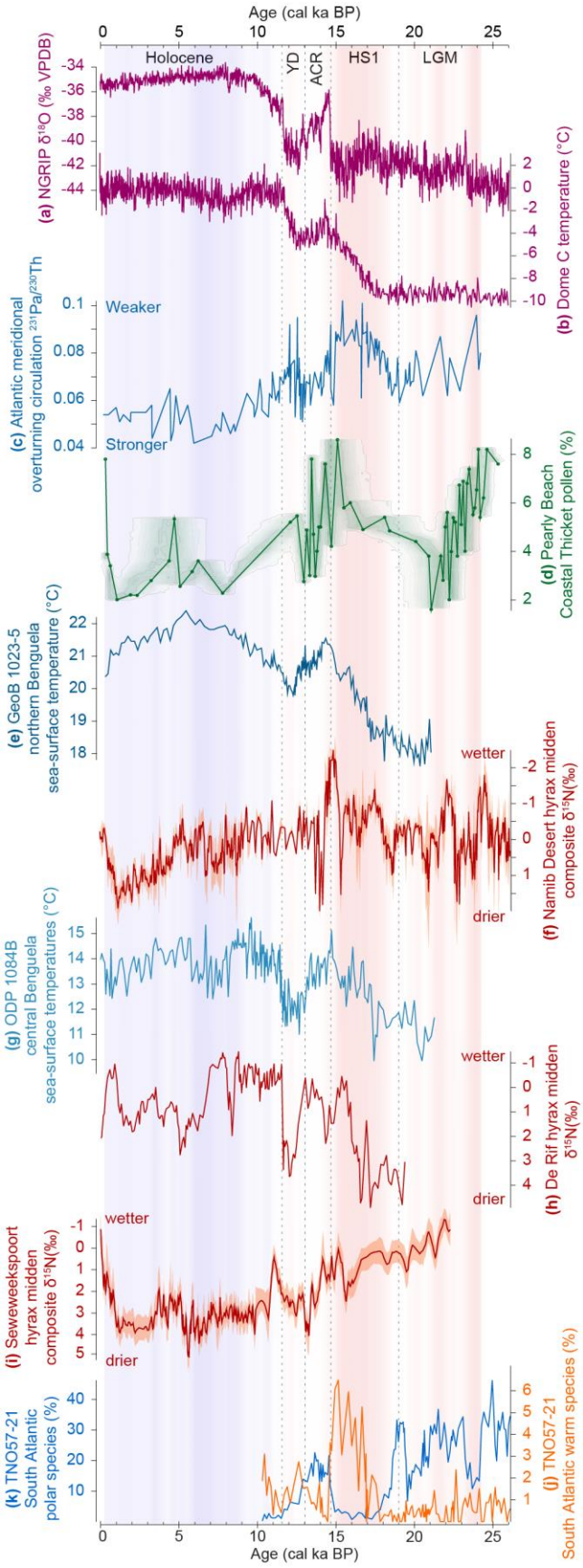

Figure 9. Comparison of records relevant to the context and climate dynamics associated with the changes observed in the Pearly Beach record. The Last Glacial Maximum (LGM), Heinrich stadial 1 (HS1), Antarctic Cold Reversal (ACR), Younger Dryas (YD) and Holocene chronozones are indicated. Shading has been added to indicate the strength of Atlantic overturning circulation relative to the 25 kyr mean (red = weaker, blue = stronger). Records shown are: **a)** North Greenland NGRIP oxygen isotope record (North Greenland Ice Core Project North Greenland Ice Core Project members, 2004), **b)** Antarctic temperature record from Dome C (Jouzel et al., 2007), **c)** record of Atlantic overturning circulation strength (Ng et al., 2018), **d)** the coastal thicket pollen record from Pearly Beach, shading from proxy ghost analysis using *rbacon* software (v. 2.3.6; Blaauw and Christen, 2011) to express chronological uncertainties, **e)** sea-surface temperature record from the GeoB 1023-5 marine core (Kim et al., 2003), **f)** Namib Desert rock hyrax midden nitrogen isotope record (Blaauw and Christen, 2011), **g)** sea-surface temperature record from ODP 1084B marine core (Farmer et al., 2005), **h)** De Rif rock hyrax midden nitrogen isotope record (Chase et al., 2011; Chase et al., 2015a), **i)** Seweweekspoort rock hyrax midden nitrogen isotope record (Chase et al., 2017), **j,k)** percentages of polar and warm water foraminiferal species in South Atlantic core TNO57-21 (Barker et al., 2009).

References

Barker, S., Diz, P., Vautravers, M.J., Pike, J., Knorr, G., Hall, I.R., Broecker, W.S., 2009. Interhemispheric Atlantic seesaw response during the last deglaciation. Nature 457, 1097-1102.

Beal, L.M., De Ruijter, W.P., Biastoch, A., Zahn, R., 2011. On the role of the Agulhas system in ocean circulation and climate. Nature 472, 429-436.

Bendle, J.M., Palmer, A.P., Thorndycraft, V.R., Matthews, I.P., 2019. Phased Patagonian Ice Sheet response to Southern Hemisphere atmospheric and oceanic warming between 18 and 17 ka. Sci Rep 9, 4133-4133.

Bergh, N.G., Cowling, R.M., 2014. Cenozoic assembly of the Greater Cape flora. Fynbos: Ecology, Evolution, and Conservation of a Megadiverse Region, 93.

Biastoch, A., Boning, C.W., Schwarzkopf, F.U., Lutjeharms, J.R.E., 2009. Increase in Agulhas leakage due to poleward shift of Southern Hemisphere westerlies. Nature 462, 495-498.

Blaauw, M., Christen, J.A., 2011. Flexible paleoclimate age-depth models using an autoregressive gamma process. Bayesian Analysis 6, 457-474.

Boucher, C., 1987. A phytosociological study of transects through the western Cape coastal foreland, South Africa. Stellenbosch University.

Boucher, C., Moll, E.J., 1981. South African mediterranean shrublands. Ecosystems of the world 11. Mediterranean-type shrublands, 233-248.

Bradshaw, P.L., Cowling, R.M., 2014. Landscapes, rock types, and climate of the Greater Cape Floristic Region. Fynbos: ecology, evolution and conservation of a megadiverse region, 26-46.

Broccoli, A.J., Dahl, K.A., Stouffer, R.J., 2006. Response of the ITCZ to Northern Hemisphere cooling. Geophys. Res. Lett. 33.

Broecker, W.S., 1998. Paleocean circulation during the last deglaciation: a bipolar seesaw? Paleoceanography 13, 119-121.

Caley, T., Giraudeau, J., Malaizé, B., Rossignol, L., Pierre, C., 2012. Agulhas leakage as a key process in the modes of Quaternary climate changes. Proceedings of the National Academy of Sciences 109, 6835-6839.

Carr, A.S., Boom, A., Chase, B.M., Meadows, M.E., Grimes, H.L., 2015. Holocene sea level and environmental change on the west coast of South Africa: evidence from plant biomarkers, stable isotopes and pollen. Journal of Paleolimnology 53, 415-432.

Carr, A.S., Thomas, D.S.G., Bateman, M.D., 2006a. Climatic and sea level controls on late Quaternary eolian activity on the Agulhas Plain, South Africa. Quaternary Research 65, 252-263.

Carr, A.S., Thomas, D.S.G., Bateman, M.D., Meadows, M.E., Chase, B., 2006b. Late Quaternary palaeoenvironments of the winter-rainfall zone of southern Africa: Palynological and sedimentological evidence from the Agulhas Plain. Palaeogeography, Palaeoclimatology, Palaeoecology 239, 147-165.

Cartwright, C., Parkington, J., 1997. The wood charcoal assemblages from Elands Bay Cave, Southwestern Cape: principles, procedures and preliminary interpretation. South African Archaeological Bulletin 52, 59-72.

Chase, B., Boom, A., Carr, A., Chevalier, M., Quick, L., Verboom, A., Reimer, P., 2019a. Extreme hydroclimate gradients within the western Cape Floristic region of South Africa since the Last Glacial Maximum. Quaternary Science Reviews 219, 297-307.

Chase, B., Niedermeyer, E.M., Boom, A., Carr, A.S., Chevalier, M., He, F., Meadows, M.E., Ogle, N., Reimer, P.J., 2019b. Orbital controls on Namib Desert hydroclimate over the past 50,000 years. Geology 47, 867-871.

Chase, B.M., 2010. South African palaeoenvironments during marine oxygen isotope stage 4: a context for the Howiesons Poort and Still Bay industries. Journal of Archaeological Science 37, 1359-1366.

744 Chase, B.M., Boom, A., Carr, A.S., Carré, M., Chevalier, M., Meadows, M.E., Pedro, J.B., Stager, J.C., Reimer,
745 P.J., 2015a. Evolving southwest African response to abrupt deglacial North Atlantic climate change events.
746 Quaternary Science Reviews 121, 132-136.
747 Chase, B.M., Boom, A., Carr, A.S., Meadows, M.E., Reimer, P.J., 2013. Holocene climate change in
748 southernmost South Africa: rock hyrax middens record shifts in the southern westerlies. Quaternary
749 Science Reviews 82, 199-205.
750 Chase, B.M., Boom, A., Carr, A.S., Quick, L.J., Reimer, P.J., 2020. High-resolution record of Holocene
751 climate change dynamics from southern Africa's temperate-tropical boundary, Baviaanskloof, South
752 Africa. Palaeogeography, Palaeoclimatology, Palaeoecology 539, 109518.
753 Chase, B.M., Chevalier, M., Boom, A., Carr, A.S., 2017. The dynamic relationship between temperate and
754 tropical circulation systems across South Africa since the last glacial maximum. Quaternary Science
755 Reviews 174, 54-62.
756 Chase, B.M., Lim, S., Chevalier, M., Boom, A., Carr, A.S., Meadows, M.E., Reimer, P.J., 2015b. Influence of
757 tropical easterlies in southern Africa's winter rainfall zone during the Holocene. Quaternary Science
758 Reviews 107, 138-148.
759 Chase, B.M., Meadows, M.E., 2007. Late Quaternary dynamics of southern Africa's winter rainfall zone.
760 Earth-Science Reviews 84, 103-138.
761 Chase, B.M., Meadows, M.E., Scott, L., Thomas, D.S.G., Marais, E., Sealy, J., Reimer, P.J., 2009. A record of
762 rapid Holocene climate change preserved in hyrax middens from southwestern Africa. Geology 37, 703-
763 706.
764 Chase, B.M., Quick, L.J., 2018. Influence of Agulhas forcing of Holocene climate change in South Africa's
765 southern Cape. Quaternary Research 90, 303-309.
766 Chase, B.M., Quick, L.J., Meadows, M.E., Scott, L., Thomas, D.S.G., Reimer, P.J., 2011. Late-glacial
767 interhemispheric climate dynamics revealed in South African hyrax middens. Geology 39, 19 - 22.
768 Chevalier, M., 2019. Enabling possibilities to quantify past climate from fossil assemblages at a global
769 scale. Global and Planetary Change 175, 27-35.
770 Chevalier, M., 2020. GBIF for CREST database.
771 Chevalier, M., Chase, B.M., 2015. Southeast African records reveal a coherent shift from high- to low-
772 latitude forcing mechanisms along the east African margin across last glacial–interglacial transition.
773 Quaternary Science Reviews 125, 117-130.
774 Chevalier, M., Chase, B.M., 2016. Determining the drivers of long-term aridity variability: a southern
775 African case study. Journal of Quaternary Science 31, 143-151.
776 Chevalier, M., Cheddadi, R., Chase, B.M., 2014. CREST (Climate REconstruction SofTware): a probability
777 density function (PDF)-based quantitative climate reconstruction method. Climate of the Past 10, 2081–
778 2098.
779 Clark, P.U., Dyke, A.S., Shakun, J.D., Carlson, A.E., Clark, J., Wohlfarth, B., Mitrovica, J.X., Hostetler, S.W.,
780 McCabe, A.M., 2009. The last glacial maximum. science 325, 710-714.
781 Climate System Analysis Group, U.o.C.T., 2021. Climate Information Platform. University of Cape Town.
782 Cockcroft, M.J., Wilkinson, M.J., Tyson, P.D., 1987. The application of a present-day climatic model to the
783 late Quaternary in southern Africa. Climatic Change 10, 161-181.
784 Cohen, A.L., Tyson, P.D., 1995. Sea surface temperature fluctuations during the Holocene off the south
785 coast of Africa: implications for terrestrial climate and rainfall. Holocene 5, 304-312.
786 Cordova, C.E., Kirsten, K.L., Scott, L., Meadows, M., Lücke, A., 2019. Multi-proxy evidence of late-Holocene
787 paleoenvironmental change at Princessvlei, South Africa: The effects of fire, herbivores, and humans.
788 Quaternary Science Reviews 221, 105896.
789 Cowling, R., Campbell, B., Mustart, P., McDonald, D., Jarman, M., Moll, E., 1988. Vegetation classification
790 in a floristically complex area: The Agulhas Plain. South African Journal of Botany 54, 290-300.

Cowling, R.M., 1992. The Ecology of Fynbos: Nutrients, Fire, and Diversity. Oxford University Press, Cape Town.
Cowling, R.M., 1996. Flora and vegetation of Groot Hagelkraal (Bantamsklip site), Agulhas Plain, Unpublished Report. Institute for Plant Conservation, University of Cape Town.
Cowling, R.M., Cartwright, C.R., Parkington, J.E., Allsopp, J.C., 1999. Fossil wood charcoal assemblages from Elands Bay Cave, South Africa: implications for late Quaternary vegetation and climates in the winter-rainfall fynbos biome. Journal of Biogeography 26, 367-378.
Cowling, R.M., Lombard, A.T., 2002. Heterogeneity, speciation/extinction history and climate: explaining regional plant diversity patterns in the Cape Floristic Region. Diversity and Distributions 8, 163-179.
Cowling, R.M., Potts, A.J., Bradshaw, P.L., Colville, J., Arianoutsou, M., Ferrier, S., Forest, F., Fyllas, N.M., Hopper, S.D., Ojeda, F., 2015. Variation in plant diversity in mediterranean-climate ecosystems: The role of climatic and topographical stability. Journal of Biogeography 42, 552-564.
Cowling, R.M., Richardson, D.M., Schulze, R.E., Hoffman, M.T., Midgley, J.J., Hilton-Taylor, C., 1997. Species diversity at the regional scale, in: Cowling, R.M., Richardson, D.M., Pierce, S.M. (Eds.), Vegetation of Southern Africa. Cambridge University Press, Cambridge, pp. 447 - 273.
Crowley, G.M., 1992. North Atlantic deep water cools the Southern Hemisphere. Palaeoceanography 7, 489-497.
Deacon, H.J., Deacon, J., Scholtz, A., Thackeray, J.F., Brink, J.S., 1984. Correlation of palaeoenvironmental data from the Late Pleistocene and Holocene deposits at Boomplaas Cave, southern Cape, in: Vogel, J.C. (Ed.), Late Cainozoic Palaeoclimates of the Southern Hemisphere. Balkema, Rotterdam, pp. 339-360.
Deacon, H.J., Geleijnse, V.B., Thackeray, A.I., Thackeray, J.F., Tusenius, M.L., Vogel, J.C., 1986. Late Pleistocene cave deposits in the southern Cape: current research at Klasies River. Palaeoecology of Africa. Vol. 17. Proc. 7th SASQUA conference, Stellenbosch, 1985, 31-37.
du Plessis, N., Chase, B.M., Quick, L.J., Haberzettl, T., Kasper, T., Meadows, M.E., 2020. Vegetation and climate change during the Medieval Climate Anomaly and the Little Ice Age on the southern Cape coast of South Africa: Pollen evidence from Bo Langvlei. The Holocene 0, 0959683620950444.
Dyez, K.A., Zahn, R., Hall, I.R., 2014. Multicentennial Agulhas leakage variability and links to North Atlantic climate during the past 80,000 years. Paleoceanography 29, 1238-1248.
Engelbrecht, C.J., Landman, W.A., Engelbrecht, F.A., Malherbe, J., 2015. A synoptic decomposition of rainfall over the Cape south coast of South Africa. Climate Dynamics 44, 2589-2607.
Engelbrecht, F.A., Marean, C.W., Cowling, R.M., Engelbrecht, C.J., Neumann, F.H., Scott, L., Nkoana, R., O'Neal, D., Fisher, E., Shook, E., Franklin, J., Thatcher, M., McGregor, J.L., Van der Merwe, J., Dedekind, Z., Difford, M., 2019. Downscaling Last Glacial Maximum climate over southern Africa. Quaternary Science Reviews 226, 105879.
Faegri, K., Iversen, J., 1989. Textbook of Pollen Analysis, 4th ed. John Wiley & Sons, Chichester.
Faith, J.T., Chase, B.M., Avery, D.M., 2018. Late Quaternary micromammals and the precipitation history of the southern Cape, South Africa. Quaternary Research 91, 848-860.
Faith, J.T., Chase, B.M., Avery, D.M., 2020. Late Quaternary micromammals and the precipitation history of the southern Cape, South Africa: response to comments by F. Thackeray, Quaternary Research 95, 154–156. Quaternary Research 95, 157-159.
Farmer, E.C., deMenocal, P.B., Marchitto, T.M., 2005. Holocene and deglacial ocean temperature variability in the Benguela upwelling region: implications for low-latitude atmospheric circulation. Paleoceanography 20, doi:10.1029/2004PA001049.
Fick, S.E., Hijmans, R.J., 2017. WorldClim 2: new 1-km spatial resolution climate surfaces for global land areas. International Journal of Climatology 37, 4302-4315.
GEBCO, 2012. The GEBCO_08 Grid, version 20120320.
Goldblatt, P., 1978. An analysis of the flora of southern Africa: its characteristics, relationships, and origins. Annals of the Missouri Botanical Garden 65, 369-436.

Gordon, A.L., 1986. Interocean exchange of thermocline water. Journal of Geophysical Research: Oceans 91, 5037-5046.
Gresse, P.G., Theron, J.N., 1992. The geology of the Worcester area: explanations of sheet 3319 (1:250 000). Geological Survey of South Africa, Pretoria.
Grimm, E., 1987. Coniss: A fortran 77 program for stratigraphically constrained cluster analysis by the method of incremental sum of squares. Computers and Geosciences 13, 13-35.
Grimm, E., 1991. Tilia and Tiliagraph version 1.7.16. Illinois State Museum.
Group, G.B.C., 2020. The GEBCO_2020 Grid - a continuous terrain model of the global oceans and land, in: British Oceanographic Data Centre, N.O.C., NERC, UK (Ed.).
Heaton, T.H.E., Talma, A.S., Vogel, J.C., 1986. Dissolved gas paleotemperatures and 18O variations derived from groundwater near Uitenhage, South Africa. Quaternary Research 25, 79-88.
Henshilwood, C.S., Sealy, J.C., Yates, R., Cruz-Uribe, K., Goldberg, P., Grine, F.E., Klein, R.G., Poggenpoel, C., van Niekerk, K., Watts, I., 2001. Blombos Cave, Southern Cape, South Africa: Preliminary Report on the 1992–1999 Excavations of the Middle Stone Age Levels. Journal of Archaeological Science 28, 421-448.
Hogg, A.G., Hua, Q., Blackwell, P.G., Niu, M., Buck, C.E., Guilderson, T.P., Heaton, T.J., Palmer, J.G., Reimer, P.J., Reimer, R.W., 2013. SHCal13 Southern Hemisphere Calibration, 0–50,000 cal yr BP. Radiocarbon 55, 1889-1903.
Holmgren, K., Lee-Thorp, J.A., Cooper, G.R.J., Lundblad, K., Partridge, T.C., Scott, L., Sithaldeen, R., Talma, A.S., Tyson, P.D., 2003. Persistent millennial-scale climatic variability over the past 25,000 years in Southern Africa. Quaternary Science Reviews 22, 2311-2326.
Irving, S.J.E., Meadows, M.E., 1997. Radiocarbon chronology and organic matter accumulation at Vankervelsvlei, near Knysna, South Africa. South African Geographical Journal 79, 101-105.
Jones, M.G.W., van Nieuwenhuizen, G.D.P., Day, J.A., 2002. Selecting priority wetlands for conservation measures. The Agulhas Plain as a case study, Report to CAPE (Cape Action Plan for the environment).
Jouzel, J., Masson-Delmotte, V., Cattani, O., Dreyfus, G., Falourd, S., Hoffmann, G., Minster, B., Nouet, J., Barnola, J.M., Chappellaz, J., Fischer, H., Gallet, J.C., Johnsen, S., Leuenberger, M., Loulergue, L., Luethi, D., Oerter, H., Parrenin, F., Raisbeck, G., Raynaud, D., Schilt, A., Schwander, J., Selmo, E., Souchez, R., Spahni, R., Stauffer, B., Steffensen, J.P., Stenni, B., Stocker, T.F., Tison, J.L., Werner, M., Wolff, E.W., 2007. Orbital and millennial Antarctic climate variability over the past 800,000 years. Science 317, 793-797.
Jury, M., Rouault, M., Weeks, S., Schormann, M., 1997. Atmospheric boundary-layer fluxes and structure across a land-sea transition zone in south-eastern Africa. Boundary-layer meteorology 83, 311-330.
Jury, M.R., Valentine, H.R., Lutjeharms, J.R.E., 1993. Influence of the Agulhas Current on summer rainfall along the southeast coast of South Africa. Journal of Applied Meteorology 32, 1282-1287.
Kim, J.-H., Schneider, R.R., 2003. Low-latitude control of interhemispheric sea-surface temperature contrast in the tropical Atlantic over the past 21 kyrs: the possible role of SE trade winds. Climate Dynamics 23, 337-347.
Kim, J.-H., Schneider, R.R., Mulitza, S., Müller, P.J., 2003. Reconstruction of SE trade-wind intensity based on sea-surface temperature gradients in the Southeast Atlantic over the last 25 kyr. Geophysical Research Letters 30, 2144.
Kirsten, K.L., Haberzettl, T., Wündsch, M., Frenzel, P., Meschner, S., Smit, A.J., Quick, L.J., Mäusbacher, R., Meadows, M.E., 2018. A multiproxy study of the ocean-atmospheric forcing and the impact of sea-level changes on the southern Cape coast, South Africa during the Holocene. Palaeogeography, Palaeoclimatology, Palaeoecology.
Kirsten, K.L., Kasper, T., Cawthra, H.C., Strobel, P., Quick, L.J., Meadows, M.E., Haberzettl, T., Holocene variability in climate and oceanic conditions in the winter rainfall zone of South Africa—inferred from a high resolution diatom record from Verlorenvlei. Journal of Quaternary Science n/a.

885 Kirsten, K.L., Kasper, T., Cawthra, H.C., Strobel, P., Quick, L.J., Meadows, M.E., Haberzettl, T., 2020.
886 Holocene variability in climate and oceanic conditions in the winter rainfall zone of South Africa—inferred
887 from a high resolution diatom record from Verlorenvlei. Journal of Quaternary Science 35, 572-581.
888 Kirsten, K.L., Meadows, M.E., 2016. Late-Holocene palaeolimnological and climate dynamics at
889 Princessvlei, South Africa: Evidence from diatoms. The Holocene 26, 1371-1381.
890 Klein, R.G., Cruz-Uribe, K., 2000. Middle and Later Stone Age large mammal and tortoise remains from Die
891 Kelders Cave 1, Western Cape Province, South Africa. Journal of Human Evolution 38, 169-195.
892 Lantz, H., Bremer, B., 2004. Phylogeny inferred from morphology and DNA data: characterizing well-
893 supported groups in Vanguerieae (Rubiaceae). Botanical Journal of the Linnean Society 146, 257-283.
894 Lee, S.Y., Chiang, J.C., Matsumoto, K., Tokos, K.S., 2011. Southern Ocean wind response to North Atlantic
895 cooling and the rise in atmospheric CO2: Modeling perspective and paleoceanographic implications.
896 Paleoceanography 26.
897 Lim, S., Chase, B.M., Chevalier, M., Reimer, P.J., 2016. 50,000 years of vegetation and climate change in
898 the southern Namib Desert, Pella, South Africa. Palaeogeography, Palaeoclimatology, Palaeoecology 451,
899 197-209.
900 Linder, H.P., 2005. Evolution of diversity: the Cape flora. Trends in Plant Science 10, 536-541.
901 Linder, H.P., Mann, D.M., 1998. The phylogeny and biogeography of *Thamnochortus* (Restionaceae).
902 Botanical Journal of the Linnean Society 128, 319-357.
903 Linder, H.P., Meadows, M., Cowling, R.M., 1992. History of the Cape Flora, in: Cowling, R.M. (Ed.), The
904 Ecology of Fynbos: nutrients, fire and diversity. Oxford University Press, Cape Town, pp. 113-134.
905 Lutjeharms, J., 1996. The exchange of water between the South Indian and the South Atlantic, in: Wefer,
906 G., Berger, W.H., Siedler, G., Webb, D. (Eds.), The South Atlantic: Present and Past Circulation. Springer-
907 Verlag, Berlin pp. 125 -162.
908 Malan, J.A., 1989. Bredasdorp Group, in: Johnson, M.R. (Ed.), Catalogue of South African Lithostratigraphic
909 units., 1st ed. SA Committee for Stratigraphy.
910 Marean, C.W., 2010. Pinnacle Point Cave 13B (Western Cape Province, South Africa) in context: The Cape
911 Floral kingdom, shellfish, and modern human origins. Journal of Human Evolution 59, 425-443.
912 Martin, A.R.H., 1968. Pollen analysis of Groenvlei lake sediments, Knysna (South Africa). Review of
913 Palaeobotany and Palynology 7, 107-144.
914 McManus, J.F., Francois, R., Gherardi, J.-M., Keigwin, L.D., Brown-Leger, S., 2004. Collapse and rapid
915 resumption of Atlantic meridional circulation linked to deglacial climate changes. Nature 428, 834-837.
916 Meadows, M.E., Baxter, A.J., 2001. Holocene vegetation history and palaeoenvironments at Klaarfontein
917 Springs, Western Cape, South Africa. Holocene 11, 699-706.
918 Meadows, M.E., Baxter, A.J., Parkington, J., 1996. Late Holocene environments at Verlorenvlei, Western
919 Cape Province, South Africa. Quaternary International 33, 81-95.
920 Meadows, M.E., Seliane, M., Chase, B.M., 2010. Holocene palaeoenvironments of the Cederberg and
921 Swartruggens mountains, Western Cape, South Africa: pollen and stable isotope evidence from hyrax
922 dung middens. Journal of Arid Environments 74, 786-793.
923 Meadows, M.E., Sugden, J.M., 1991. A vegetation history of the last 14,000 years on the Cederberg,
924 southwestern Cape Province. South African Journal of Science 87, 34-43.
925 Menviel, L., Spence, P., Yu, J., Chamberlain, M.A., Matear, R.J., Meissner, K.J., England, M.H., 2018.
926 Southern Hemisphere westerlies as a driver of the early deglacial atmospheric CO2 rise. Nature
927 Communications 9, 2503.
928 Mix, A.C., Ruddiman, W.F., McIntyre, A., 1986. Late Quaternary paleoceanography of the tropical Atlantic,
929 2: The seasonal cycle of sea surface temperatures, 0-20,000 years B.P. Paleoceanography 1.
930 Mooney, S.D., Tinner, W., 2011. The analysis of charcoal in peat and organic sediments. Mires and Peat 7,
931 1-18.

Moore, P.D., Webb, J.A., Collinson, M.E., 1991. Pollen Analysis, 2nd ed. Blackwell Scientific Publications, Oxford.
Mucina, L., Adams, J.B., Knevel, I.C., Rutherford, M.C., Powrie, L.W., Bolton, J.J., van der Merwe, J.H., Anderson, R.J., Bornman, T.G., le Roux, A., 2006a. Coastal vegetation of South Africa. The vegetation of South Africa, Lesotho and Swaziland, 658-697.
Mucina, L., Geldenhuys, C.J., 2006. Afrotemperate, subtropical and azonal forests., in: Mucina, L., Rutherford, M.C. (Eds.), The vegetation of South Africa, Lesotho and Swaziland. South African National Biodiversity Institute, Pretoria, South Africa.
Mucina, L., Rutherford, M.C., 2006. The vegetation of South Africa, Lesotho and Swaziland, Strelitzia. South African National Biodiversity Institute, Pretoria.
Mucina, L., Rutherford, M.C., Powrie, L.M., 2006b. Inland Azonal Vegetation, in: Mucina, L., Rutherford, M.C. (Eds.), The Vegetation of South Africa, Lesotho and Swaziland. South African National Biodiversity Institute, Pretoria, pp. 617-657.
Mustart, P.J., Cowling, R.M., Albertyn, J., 2003. Southern Overberg South African Wild Flower Guide 8. Botanical Society of South Africa, Cape Town.
Nakagawa, T., Brugiapaglia, E., Digerfeldt, G., Reille, M., De Beaulieu, J.-L., Yasuda, Y., 1998. Dense media separation as a more efficient pollen extraction method for use with organic sediment/deposit samples: comparison with the conventional method. Boreas 27, 15-24.
Neumann, F.H., Scott, L., Bamford, M.K., 2011. Climate change and human disturbance of fynbos vegetation during the late Holocene at Princess Vlei, Western Cape, South Africa. The Holocene 21, 1137-1149.
Ng, H.C., Robinson, L.F., McManus, J.F., Mohamed, K.J., Jacobel, A.W., Ivanovic, R.F., Gregoire, L.J., Chen, T., 2018. Coherent deglacial changes in western Atlantic Ocean circulation. Nature Communications 9, 1-10.
Nielsen, S.H., Koç, N., Crosta, X., 2004. Holocene climate in the Atlantic sector of the Southern Ocean: controlled by insolation or oceanic circulation? Geology 32, 317-320.
North Greenland Ice Core Project members, 2004. High-resolution record of Northern Hemisphere climate extending into the last interglacial period. Nature 431, 147-151.
Nzunda, E., Lawes, M., 2011. Costs of resprouting are traded off against reproduction in subtropical coastal dune forest trees. Plant Ecology 212, 1991-2001.
Parkington, J., Cartwright, C., Cowling, R.M., Baxter, A., Meadows, M., 2000. Palaeovegetation at the Last Glacial Maximum in the Western Cape, South Africa: wood charcoal and pollen evidence from Elands Bay Cave. South African Journal of Science 96, 543-546.
Parkington, J.E., Poggenpoel, C., Buchanan, W.F., Robey, T., Manhire, A.H., Sealy, J., 1988. Holocene coastal settlement patterns in the Western Cape, in: Bailey, G., Parkington, J.E. (Eds.), The archaeology of prehistoric coastlines. Cambridge University Press, Cambridge, pp. 22-41.
Patterson, W.A., Edwards, K.J., Maguire, D.J., 1987. Microscopic charcoal as a fossil indicator of fire. Quaternary Science Reviews 6, 3-23.
Pedro, J.B., Bostock, H.C., Bitz, C.M., He, F., Vandergoes, M.J., Steig, E.J., Chase, B.M., Krause, C.E., Rasmussen, S.O., Markle, B.R., 2016. The spatial extent and dynamics of the Antarctic Cold Reversal. Nature Geoscience 9, 51-55.
Pedro, J.B., van Ommen, T.D., Rasmussen, S.O., Morgan, V.I., Chappellaz, J., Moy, A.D., Masson-Delmotte, V., Delmotte, M., 2011. The last deglaciation: timing the bipolar seesaw. Climates of the Past 7, 671-683.
Peeters, F.J.C., Acheson, R., Brummer, G.-J.A., de Ruijter, W.P.M., Schneider, R.R., Ganssen, G.M., Ufkes, E., Kroon, D., 2004. Vigorous exchange between the Indian and Atlantic oceans at the end of the past five glacial periods. Nature 430, 661-665.

Quick, L.J., Carr, A.S., Meadows, M.E., Boom, A., Bateman, M.D., Roberts, D.L., Reimer, P.J., Chase, B.M., 2015. A late Pleistocene–Holocene multi-proxy record of palaeoenvironmental change from Still Bay, southern Cape Coast, South Africa. Journal of Quaternary Science 30, 870-885.
Quick, L.J., Chase, B.M., Meadows, M.E., Scott, L., Reimer, P.J., 2011. A 19.5 kyr vegetation history from the central Cederberg Mountains, South Africa: Palynological evidence from rock hyrax middens. Palaeogeography, Palaeoclimatology, Palaeoecology 309, 253-270.
Quick, L.J., Chase, B.M., Wündsch, M., Kirsten, K.L., Chevalier, M., Mäusbacher, R., Meadows, M.E., Haberzettl, T., 2018. A high-resolution record of Holocene climate and vegetation dynamics from the southern Cape coast of South Africa: pollen and microcharcoal evidence from Eilandvlei. Journal of Quaternary Science 33, 487-500.
Quick, L.J., Meadows, M.E., Bateman, M.D., Kirsten, K.L., Mäusbacher, R., Haberzettl, T., Chase, B.M., 2016. Vegetation and climate dynamics during the last glacial period in the fynbos-afrotemperate forest ecotone, southern Cape, South Africa. Quaternary International 404, 136–149.
Rahmstorf, S., 2006. Thermohaline ocean circulation. Encyclopedia of quaternary sciences 5.
Reason, C.J.C., 2001. Evidence for the influence of the Agulhas Current on regional atmospheric circulation patterns. Journal of Climate 14, 2769-2778.
Reason, C.J.C., Landman, W., Tennant, W., 2006. Seasonal to decadal prediction of southern African climate and its links with variability of the Atlantic ocean. Bulletin of the American Meteorological Society 87, 941-955.
Reason, C.J.C., Rouault, M., Melice, J.L., Jagadheesha, D., 2002. Interannual winter rainfall variability in SW South Africa and large scale ocean-atmosphere interactions. Meteorology and Atmospheric Physics 80, 19-29.
Rebelo, A.G., Boucher, C., Helme, N., Mucina, L., Rutherford, M.C., 2006. Fynbos Biome, in: Mucina, L., Rutherford, M.C. (Eds.), The vegetation of South Africa, Lesotho and Swaziland. South African National Biodiversity Institute, Pretoria, pp. 221-299.
Rebelo, A.G., Cowling, R.M., Campbell, B.M., Meadows, M.E., 1991. Plant communities of the Riversdale Plain. . South African Journal of Botany 57, 10–28.
Rector, A.L., Reed, K.E., 2010. Middle and late Pleistocene faunas of Pinnacle Point and their paleoecological implications. Journal of Human Evolution 59, 340-357.
Reynolds, R.W., Smith, T.M., Liu, C., Chelton, D.B., Casey, K.S., Schlax, M.G., 2007. Daily High-Resolution-Blended Analyses for Sea Surface Temperature. Journal of Climate 20, 5473-5496.
Ritz, S.P., Stocker, T.F., Grimalt, J.O., Menviel, L., Timmermann, A., 2013. Estimated strength of the Atlantic overturning circulation during the last deglaciation. Nature geoscience 6, 208-212.
Rouault, M., Florenchie, P., Fauchereau, N., Reason, C.J., 2003. South East tropical Atlantic warm events and southern African rainfall. Geophysical Research Letters 30.
Rühs, S., Schwarzkopf, F., Speich, S., Biastoch, A., 2019. Cold vs. warm water route–sources for the upper limb of the Atlantic Meridional Overturning Circulation revisited in a high-resolution ocean model. Ocean Science 15, 489-512.
SANBI, 2003. PRECIS (National Herbarium Pretoria (PRE) Computerized Information System) database, in: Institute, S.A.N.B. (Ed.).
Schalke, H.J.W.G., 1973. The Upper Quaternary of the Cape Flats area. Scripta Geologica 15, 1-57.
Scholtz, A., 1986. Palynological and Palaeobotanical Studies in the Southern Cape. University of Stellenbosch, Stellenbosch, South Africa.
Schweitzer, F.R., Wilson, M.L., 1982. Byneskranskop 1, a late Quaternary living site in the southern Cape Province, South Africa: A Late Quaternary Living Site in the Southern Cape Province, South Africa. South African Museum.
Scott, L., 1982. Late Quaternary fossil pollen grains from the Transvaal, South Africa. Review of Palaeobotany and Palynology 36, 241-278.

Scott, L., Woodborne, S., 2007a. Pollen analysis and dating of Late Quaternary faecal deposits (hyraceum) in the Cederberg, Western Cape, South Africa. Review of Palaeobotany and Palynology 144, 123-134.
Scott, L., Woodborne, S., 2007b. Pollen analysis and dating of late Quaternary faecal deposits (hyraceum) in the Cederberg, Western Cape, South Africa. Review of Palaeobotany and Palynology 144, 123-134.
Scott, L., Woodborne, S., 2007c. Vegetation history inferred from pollen in Late Quaternary faecal deposits (hyraceum) in the Cape winter-rain region and its bearing on past climates in South Africa. Quaternary Science Reviews 26, 941-953.
Spratt, R.M., Lisiecki, L.E., 2016. A Late Pleistocene sea level stack. Climate of the Past 12, 1079-1092.
Stager, J.C., Mayewski, P.A., White, J., Chase, B.M., Neumann, F.H., Meadows, M.E., King, C.D., Dixon, D.A., 2012. Precipitation variability in the winter rainfall zone of South Africa during the last 1400 yr linked to the austral westerlies. Climates of the Past 8, 877-887.
Stocker, T.F., 1998. The seesaw effect. Science 282, 61-62.
Stocker, T.F., Johnsen, S.J., 2003. A minimum thermodynamic model for the bipolar seesaw. Paleoceanography 18.
Stockmarr, J., 1973. Determination of spore concentration with an electronic particle counter. Danmarks geologiske undersøgelse Arbog, 87–89.
Stuiver, M., Polach, H.A., 1977. Discussion: reporting of ^{14}C data. Radiocarbon 19, 355-363.
Stute, M., Talma, A.S., 1998. Glacial temperatures and moisture transport regimes reconstructed from noble gas and $\delta^{18}O$, Stampriet aquifer, Namibia, Isotope Techniques in the Study of Past and Current Environmental Changes in the Hydrosphere and the Atmosphere. IAEA Vienna Symposium 1997, Vienna, pp. 307-328.
Taljaard, J., 1996. Atmospheric Circulation Systems, Synoptic Climatology and Weather Phenomena of South Africa. South African Weather Service Technical Paper 32. South African Weather Service, Pretoria, South Africa.
Talma, A.S., Vogel, J.C., 1992. Late Quaternary paleotemperatures derived from a speleothem from Cango Caves, Cape Province, South Africa. Quaternary Research 37, 203-213.
Thackeray, J.F., 2020. Late Quaternary micromammals and the precipitation history of the southern Cape, South Africa—comment on the published paper by Faith et al., Quaternary Research (2019), Vol. 91, 848–860. Quaternary Research 95, 154-156.
Thwaites, R.N., Cowling, R.M., 1988. Soil-vegetation relationships on the Agulhas Plain, South Africa. Catena 15, 333-345.
Todd, M., Washington, R., 1999. Circulation anomalies associated with tropical-temperate troughs in southern Africa and the south west Indian Ocean. Climate Dynamics 15, 937-951.
Trabucco, A., Zomer, R.J., 2019. Global Aridity Index and Potential Evapotranspiration (ET0) Climate Database v2. . https://figshare.com/articles/Global_Aridity_Index_and_Potential_Evapotranspiration_ET0_Climate_Database_v2/7504448/3.
Truc, L., Chevalier, M., Favier, C., Cheddadi, R., Meadows, M.E., Scott, L., Carr, A.S., Smith, G.F., Chase, B.M., 2013. Quantification of climate change for the last 20,000 years from Wonderkrater, South Africa: Implications for the long-term dynamics of the Intertropical Convergence Zone. Palaeogeography, Palaeoclimatology, Palaeoecology 386, 575-587.
Tyson, P.D., 1986. Climatic Change and Variability in Southern Africa. Oxford University Press, Cape Town.
Tyson, P.D., Preston-Whyte, R.A., 2000. The Weather and Climate of Southern Africa. Oxford University Press, Cape Town.
Valsecchi, V., Chase, B.M., Slingsby, J.A., Carr, A.S., Quick, L.J., Meadows, M.E., Cheddadi, R., Reimer, P.J., 2013. A high resolution 15,600-year pollen and microcharcoal record from the Cederberg Mountains, South Africa. Palaeogeography, Palaeoclimatology, Palaeoecology 387, 6-16.

van Zinderen Bakker, E.M., 1953. South African pollen grains and spores. Volume I. Balkema, Amsterdam–Cape Town.
van Zinderen Bakker, E.M., 1956. South African pollen grains and spores. Volume II. Balkema, Amsterdam–Cape Town.
van Zinderen Bakker, E.M., 1976. The evolution of late Quaternary paleoclimates of Southern Africa. Palaeoecology of Africa 9, 160-202.
van Zinderen Bakker, E.M., Coetzee, J.A., 1959. South African pollen grains and spores. Volume III. Balkema, Amsterdam–Cape Town.
Walker, N., 1990. Links between South African summer rainfall and temperature variability of the Agulhas and Benguela Current systems. Journal of Geophysical Research: Oceans 95, 3297-3319.
Walker, N.D., Shillington, F.A., 1990. The effect of oceanographic variability on the South African weather and climate. South African Journal of Science 86, 382-386.
Willis, C.K., Cowling, R.M., Lombard, A.T., 1996. Patterns of endemism in the limestone flora of South African lowland fynbos. Biodiversity and Conservation 5, 55-73.
Wündsch, M., Haberzettl, T., Cawthra, H.C., Kirsten, K.L., Quick, L.J., Zabel, M., Frenzel, P., Hahn, A., Baade, J., Daut, G., Kasper, T., Meadows, M.E., Mäusbacher, R., 2018. Holocene environmental change along the southern Cape coast of South Africa – Insights from the Eilandvlei sediment record spanning the last 8.9 kyr. Global and Planetary Change 163, 51-66.
Wündsch, M., Haberzettl, T., Kirsten, K.L., Kasper, T., Zabel, M., Dietze, E., Baade, J., Daut, G., Meschner, S., Meadows, M.E., Mäusbacher, R., 2016. Sea level and climate change at the southern Cape coast, South Africa, during the past 4.2 kyr. Palaeogeography, Palaeoclimatology, Palaeoecology 446, 295-307.
Zomer, R.J., Trabucco, A., Bossio, D.A., van Straaten, O., Verchot, L.V., 2008. Climate Change Mitigation: A Spatial Analysis of Global Land Suitability for Clean Development Mechanism Afforestation and Reforestation. Agriculture, Ecosystems and Environment 126, 67-80.